Max-Planck-Institut
für Meteorologie

REPORT No. 161

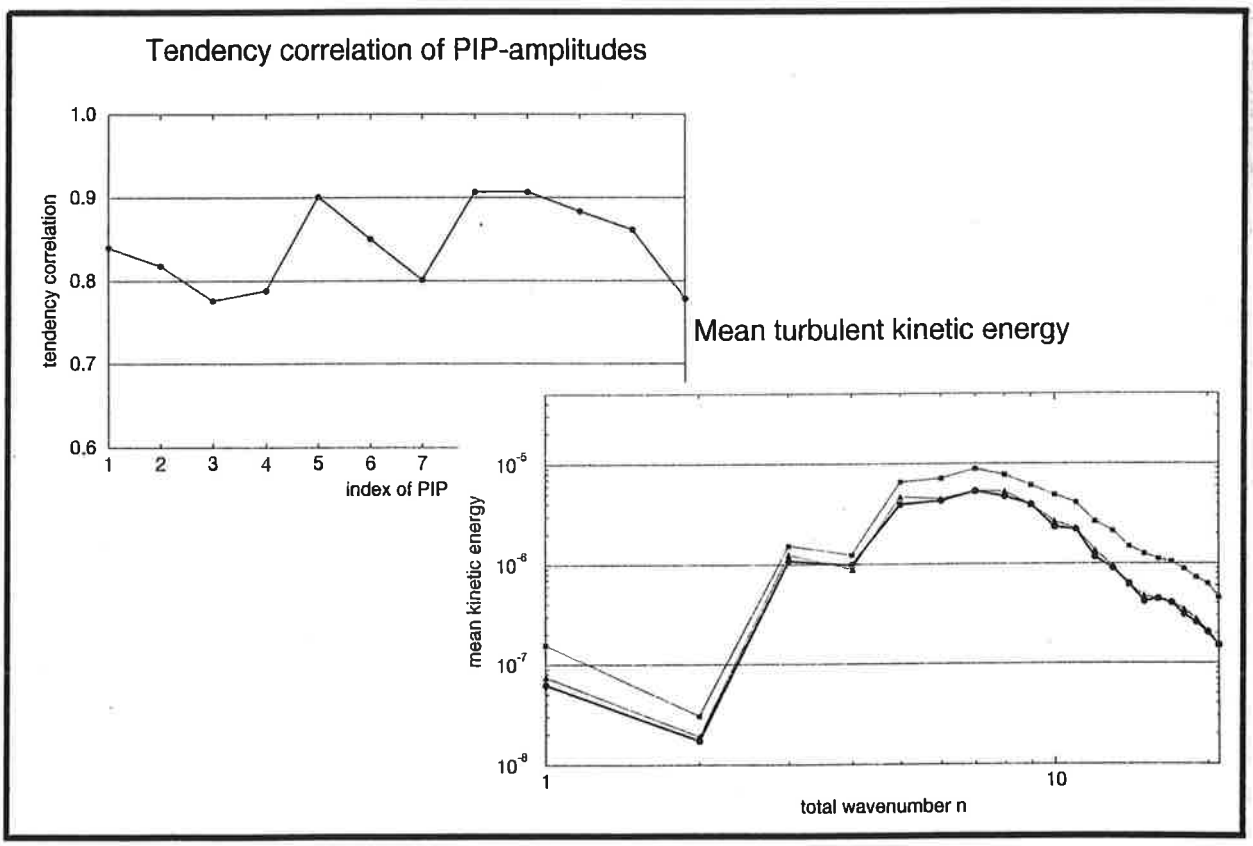

THE REDUCTION OF COMPLEX DYNAMICAL SYSTEMS USING PRINCIPAL INTERACTION PATTERNS

by

FRANK KWASNIOK

HAMBURG, May 1995

AUTHOR:

Frank Kwasniok

Max-Planck-Institut
für Meteorologie

MAX-PLANCK-INSTITUT
FÜR METEOROLOGIE
BUNDESSTRASSE 55
D-20146 Hamburg
F.R. GERMANY

Tel.: +49-(0)40-4 11 73-0
Telefax: +49-(0)40-4 11 73-298
E-Mail: <name> @ dkrz.d400.de

The Reduction of Complex Dynamical Systems Using Principal Interaction Patterns

F. Kwasniok
Max-Planck-Institut für Meteorologie
Bundesstr. 55, D-20146 Hamburg, Germany

May 5, 1995

ISSN 0937-1060

Abstract

A method of constructing low-dimensional nonlinear models capturing the main features of complex dynamical systems with many degrees of freedom is described. The system is projected onto a linear subspace spanned by only a few characteristic spatial structures called Principal Interaction Patterns (PIPs). The expansion coefficients are assumed to be governed by a nonlinear dynamical system. The optimal low-dimensional model is determined by identifying spatial modes and interaction coefficients describing their time evolution simultaneously according to a nonlinear variational principle.

The algorithm is applied to a two-dimensional geophysical fluid system on the sphere. The models based on Principal Interaction Patterns are compared to models using Empirical Orthogonal Functions (EOFs) as basis functions. A PIP-model using 12 patterns is capable of capturing the long-term behaviour of the complete system monitored by second-order statistics, while in the case of EOFs 17 modes are necessary.

1 Introduction

In various fields of research such as fluid dynamics, atmospheric science and other physical subjects there occur complex dynamical systems with many degrees of freedom. Frequently a model is formulated in terms of partial differential equations (PDEs) from which a system of ordinary differential equations (ODEs) is derived via a Galerkin procedure using eigenfunctions of some linear differential operator, commonly Fourier modes, as basis functions. Despite the complexity the dynamics of such systems are often confined to attractor sets of a dimension much smaller than the dimension of phase space. Coherent structures emerge; the dynamical behaviour of the system (or at least of an important part of the system representing e. g. a particular physical phenomenon one focuses on) seems to be dominated by the interaction among relatively few characteristic spatial patterns; i. e. the system is in fact in some sense low-dimensional. Hence the construction of minimal models capturing the principal properties of the complete system is an interesting task in such cases. Reduced models especially may be a helpful tool to understand the system, e. g. to gain insight in the physical driving mechanisms of particular phenomena occurring in the system. The Fourier modes in principle allow for a complete description of the time evolution, but this description cannot be expected to be very efficient as to the number of functions involved since Fourier modes are completely general and do not take advantage of information about the particular system under consideration at all. This leads to the idea that a description in terms of characteristic patterns may be more adequate when searching for a minimal model.

How to identify such patterns is far from clear. Modes obtained from an Empirical Orthogonal Function analysis, also referred to as Principal Component analysis, Proper Orthogonal Decomposition or Karhunen-Loève expansion in the continuous case are an obvious candidate on intuitive grounds. They can be calculated quite easily as solutions of an eigenvalue problem or of a linear Fredholm integral equation in the continous case involving second-order correlation tensors of the dynamical variables. Empirical Orthogonal Functions (EOFs) provide an optimal representation of a multivariate dynamical field in a mean least-squares sense using a given number of modes. But they a priori do not contain any information about the time evolution or the dynamical structure of the system. Of course the modes obtained from an EOF-analysis can be used and have been used [1]-[7] to build a low-dimensional model, but they are not optimized for this purpose. In [8] the EOF approach is extended to the so called Sobolev eigenfunctions. They yield an optimal representation not only of the state itself but also of its spatial derivatives by minimizing a weighted norm containing the EOFs as a special case. But still only second-order statistics is used.

In the present paper modes which are optimal with respect to the time evolution are calculated to construct reduced models. They are obtained from a nonlinear minimization procedure based on a dynamical optimality criterion involving higher-order correlation tensors of both the state variables and their time derivatives. The method takes into account spatial as well as temporal features of the dynamical system by identifying spatial modes and interaction coefficients describing their time evolution simultaneously, in contrast to EOF-analysis which concentrates solely on spatial properties of the system and does not deal with mode interaction.

The approach pursued in this paper is similar to that described in [9] and [10] which

aims at the analysis of mode interaction in the vicinity of critical points and refers to the theory of synergetics involving unstable and enslaved stable modes and corresponding order parameters. In [11] the concept of Principal Interaction Patterns is applied successfully to the description and analysis of the time evolution of baroclinic wave life cycles, a nonlinear periodic scenario in the field of atmospheric science.

The present study starts out from a chaotic two-dimensional fluid system on the rotating sphere, a crude model of the large-scale atmospheric circulation, described by a system of very many ODEs derived from a PDE via a Fourier-Galerkin procedure. The question is addressed to what extent a system with relatively few degrees of freedom using optimized basis functions succeeds in capturing the essential dynamical behaviour of the full system. The paper is organized as follows : In section 2 the methodology is outlined in general. Then the geophysical fluid system used as an example to test and study the method is introduced. The Galerkin procedure to derive reduced systems from this equation is described. In section 5 the method of constructing an optimal low-dimensional system is given in detail. Then the results are presented in section 6. Some emphasis is put on the comparison with reduced models based on EOFs. The paper is concluded in section 7. In the appendix some numerical details of the algorithm are discussed.

2 Methodology

The algorithm follows a general concept proposed by Hasselmann [12] which is slightly modified in this study. Consider a nonlinear autonomous dynamical system of first order in N-dimensional phase space :

$$\dot{\Phi} = F(\Phi) \qquad \Phi = (\Phi_1, \cdots, \Phi_N) \tag{1}$$

N may be quite large ($10^2 - 10^5$); e. g. think of a system of differential equations originating from a partial differential equation via a Galerkin procedure (cf. section 4.1). The high-dimensional dynamical field $\Phi(t)$ is projected onto a limited number of time-independent spatial modes which will be called Principal Interaction Patterns (PIPs):

$$\Phi(t) = \sum_{i=1}^{L} z_i(t)\, p_i + \rho \qquad L << N \tag{2}$$

ρ denotes the vector of the residual error. In matrix notation eq. (2) reads

$$\Phi = Pz + \rho \tag{3}$$

where P is the $(N \times L)$-matrix with the PIPs as its columns. The time dependence is suppressed in the notation from now on. For a given set of patterns the vector of expansion coefficients z at each time is defined by requiring that the squared error in the representation of the state vector

$$\rho^t M \rho = (\Phi - Pz)^t M (\Phi - Pz) \tag{4}$$

measured in some metric M be minimized. This constitutes a linear least-squares problem which can be solved uniquely using the Moore-Penrose generalized inverse of P with respect to M

$$z = P^+ \Phi = (P^t M P)^{-1} P^t M \Phi \tag{5}$$

or in other terms

$$z = P^{*t} M \Phi \tag{6}$$

with P^* being the $(N \times L)$-matrix of adjoint patterns

$$P^* = P(P^t M P)^{-1} \tag{7}$$

defined as the set of vectors p_i^* which lie in the linear subspace spanned by the PIPs and which are orthonormal to them with respect to the metric M :

$$p_i^{*t} M p_j = \delta_{ij} \tag{8}$$

The dynamics of the time-dependent coefficients z are assumed to be governed by an autonomous system of L first-order differential equations

$$\dot{z}^{\mathrm{PIP}} = G(z;\sigma) \tag{9}$$

depending on a set of adjustable parameters $\sigma = (\sigma_1, \cdots, \sigma_r)$. The dynamical system is specified as a member of a model class suitably chosen based on some physical knowledge or reasoning about the character of the system to model. $\dot{z}^{\mathrm{PIP}}$ denotes the vector of the tendencies of the PIP-amplitudes as given by the low-dimensional PIP-model in contradistinction from the tendencies given by the full system $\dot{z} = P^+\dot{\Phi} = P^+ F(\Phi)$. The optimal set of patterns and the optimal parameters are determined simultaneously by minimizing the error in the derivative of the PIP-coefficients between the reduced system and the entire system in a mean least-squares sense :

$$\begin{aligned} Q(P,\sigma) &= \overline{(\dot{z}^{\mathrm{PIP}} - \dot{z})^t \tilde{M} (\dot{z}^{\mathrm{PIP}} - \dot{z})} \\ &= \overline{\left[G(z(P),\sigma) - P^+\dot{\Phi}\right]^t \tilde{M} \left[G(z(P),\sigma) - P^+\dot{\Phi}\right]} = \mathrm{Min.} \end{aligned} \tag{10}$$

The overbar denotes ensemble averaging which is equivalent to time averaging if ergodicity is assumed. In practice it will be replaced by a sum over a discrete and finite time series obtained from a long-term integration of the full system of eq.(1). The metric $\tilde{M}$ may be chosen as the inverse of the covariance matrix of the derivatives of the PIP-amplitudes to guarantee equal weighting of all modes :

$$\tilde{M} = (P^+ \Pi P^{+^t})^{-1} = P^t M P (P^t M \Pi M P)^{-1} P^t M P \tag{11}$$

Π is the covariance matrix of the derivatives of the full system :

$$\Pi_{\alpha\beta} = \overline{\dot{\Phi}_\alpha \dot{\Phi}_\beta} \qquad \alpha, \beta = 1, \cdots, N \tag{12}$$

In principle the parameters σ are independent variables in the minimization problem. However, in this study as a first step they will be (mainly) connected to the patterns by a projection procedure (cf. section 4.2). Eq. (10) in general (if G is nonlinear) poses a high-dimensional nonlinear minimization problem which has to be solved numerically by iterative techniques.

3 The two-dimensional fluid system

In this study a vertically homogeneous layer of incompressible fluid over topography on the rotating sphere is considered. If the approximations of shallowness and quasigeostrophy are applied the flow can be described by a streamfunction $\Psi(\lambda,\mu)$ which obeys the non-divergent barotropic quasigeostrophic potential vorticity equation :

$$\frac{\partial}{\partial t}(\Delta\Psi - \frac{1}{R^2}\Psi) + \mathcal{J}(\Psi, \Delta\Psi + f + h) = -\kappa_1\Delta\Psi - \kappa_2\Delta^4\Psi + \Delta\tilde{\Psi} \tag{13}$$

λ and $\mu = \sin\theta$ denote the longitudinal and latitudinal coordinates on the sphere, respectively. Δ and $\mathcal{J}$ stand for the Laplacian and the Jacobian operator, respectively:

$$\Delta = \frac{1}{1-\mu^2}\frac{\partial^2}{\partial\lambda^2} + \frac{\partial}{\partial\mu}\left[(1-\mu^2)\frac{\partial}{\partial\mu}\right] \tag{14}$$

$$\mathcal{J}(a,b) = \frac{\partial a}{\partial\lambda}\frac{\partial b}{\partial\mu} - \frac{\partial a}{\partial\mu}\frac{\partial b}{\partial\lambda} \tag{15}$$

$f = 2\mu$ is the Coriolis parameter. h represents an effective topography which is related to the real dimensional topography of the earth $h_{\rm dim}$ by $h = 2\sin(\theta_0)A_0\frac{h_{\rm dim}}{H}$; θ_0 being some average latitude taken to be 45°N; H being a scale height of the atmosphere (H=10 km) and A_0 being a scaling factor set to 0.2. The linear damping represents surface friction; the coefficient κ_1 is assigned a value corresponding to a damping time scale of 15 days. The scale selective horizontal diffusion term parametrizes the effect of eddies on very small non-resolved spatial scales onto the resolved scales (cf. section 4.1). $\tilde{\Psi}$ is a constant forcing streamfunction which can be interpreted as thermal forcing owing to solar radiation. The Rossby radius of deformation R is set to infinity in this study (rigid lid approximation).
The zonal and meridional velocity of the flow, respectively, is given by $u = -\sqrt{1-\mu^2}\frac{\partial\Psi}{\partial\mu}$ and $v = \frac{1}{\sqrt{1-\mu^2}}\frac{\partial\Psi}{\partial\lambda}$. $\zeta = \Delta\Psi$ is the relative vorticity. Eq. (13) has been nondimensionalized using the radius of the earth as unit of length and the inverse of the angular velocity of the earth as unit of time. The barotropic vorticity equation may be regarded as the crudest model of large-scale atmospheric dynamics. For a rigorous derivation of eq. (13) from the three-dimensional Navier-Stokes equations see e. g. [13]-[15].

It can be shown that eq.(13) in the absence of friction and forcing conserves kinetic energy

$$E_{\rm kin} = \frac{1}{2}(<u,u> + <v,v>) = -\frac{1}{2}<\Psi, \Delta\Psi> \tag{16}$$

and in the absence of friction, forcing and topography conserves enstrophy

$$ENS = \frac{1}{2}<\zeta,\zeta> = \frac{1}{2}<\Delta\Psi, \Delta\Psi> \tag{17}$$

where $<\cdots,\cdots>$ signifies the scalar product

$$<a,b> = \frac{1}{4\pi}\int a^*(\lambda,\mu)b(\lambda,\mu)\,d\Omega = \frac{1}{4\pi}\int_{-1}^{1}\int_{0}^{2\pi} a^*(\lambda,\mu)b(\lambda,\mu)\,d\lambda d\mu\,. \tag{18}$$

The asterisk stands for the complex conjugate.

4 Derivation of truncated models

4.1 Spectral basis

The streamfunction, the topography and the forcing are expanded into a triangularly truncated series of spherical harmonics. The vorticity equation is considered on the Northern hemisphere. Hence only modes with odd parity are used in the expansion. This corresponds to the boundary condition $v = 0$ at the equator (no flow across the equator). For the streamfunction the expansion reads :

$$\Psi(\lambda,\mu,t) = \sum_{n=1}^{n_{max}} \sum_{m=-n}^{+n} \Psi_n^m(t)\, Y_n^m(\lambda,\mu) \qquad (n+m \text{ odd}) \tag{19}$$

$$Y_n^m(\lambda,\mu) = P_n^m(\mu)\, e^{im\lambda} \tag{20}$$

P_n^m denote associated Legendre functions of the first kind defined by

$$P_n^m(\mu) = \sqrt{(2n+1)\frac{(n-m)!}{(n+m)!}}\ \frac{(1-\mu^2)^{\frac{m}{2}}}{2^n\, n!} \left(\frac{d}{d\mu}\right)^{n+m} (\mu^2-1)^n \qquad m \geq 0 \tag{21}$$

$$P_n^{-m}(\mu) = P_n^m(\mu)$$

normalized in a way that

$$< Y_{n'}^{m'}, Y_n^m >= \delta_{nn'}\, \delta_{mm'} \tag{22}$$

holds. The spherical harmonics are eigenfunctions of the Laplacian operator :

$$\Delta Y_n^m = -n(n+1) Y_n^m \tag{23}$$

In spectral space eq. (13) reads

$$\begin{aligned} \dot{\Psi}_n^m \;=\; & \frac{1}{n(n+1)} \left[2im\Psi_n^m + \sum_{l=1}^{n_{max}} \sum_{q=-l}^{+l} \sum_{r=1}^{n_{max}} \sum_{s=-r}^{+r} \left[l(l+1) - r(r+1) \right] I_{n\,l\,r}^{m\,q\,s} \Psi_l^q \Psi_r^s \right. \\ & \left. + \sum_{l=1}^{n_{max}} \sum_{q=-l}^{+l} \sum_{r=1}^{n_{max}} \sum_{s=-r}^{+r} I_{n\,l\,r}^{m\,q\,s} \left(\Psi_l^q h_r^s - \Psi_r^s h_l^q \right) \right] \\ & -\kappa_1 \Psi_n^m - \kappa_2 [n(n+1)]^3\, \Psi_n^m + \tilde{\Psi}_n^m \end{aligned} \qquad \begin{array}{ll} n+m & \text{odd} \\ l+q & \text{odd} \\ r+s & \text{odd} \end{array} \tag{24}$$

I being the coupling integral

$$I_{n\,l\,r}^{m\,q\,s} = < Y_n^m, \mathcal{J}(Y_l^q, Y_r^s) >= \frac{1}{4\pi} \int Y_n^{-m} \mathcal{J}(Y_l^q, Y_r^s) d\Omega = \left\{ \begin{array}{ll} iK_{n\,l\,r}^{m\,q\,s} & \text{if} \quad m = q+s \\ 0 & \text{if} \quad m \neq q+s \end{array} \right\} \tag{25}$$

$$K_{n\,l\,r}^{m\,q\,s} = \frac{1}{2} \int_{-1}^{+1} P_n^m \left(q P_l^q \frac{dP_r^s}{d\mu} - s P_r^s \frac{dP_l^q}{d\mu} \right) d\mu \tag{26}$$

The summation in eq. (24) has to be taken nonredundant, i. e. only distinct combinations of pairs of wavenumbers (l,q) and (r,s) occur. K obeys the redundancy relations

$$K_{n\,l\,r}^{m\,q\,s} = K_{n\,l\,r}^{-m\,q\,s} = -K_{n\,r\,l}^{m\,s\,q} = -K_{n\;\;l\;\;r}^{-m\;-q\;-s} \tag{27}$$

and

$$K_{n\,l\,r}^{m\,q\,s} = K_{l\,n\,r}^{q\,m\,-s} = K_{r\,l\,n}^{s\,-q\,m}\,. \tag{28}$$

The latter ones may be established by integration by parts [16]. $I_{n\,l\,r}^{m\,q\,s}$ vanishes unless the wavevectors (n,m), (l,q) and (r,s) satisfy certain selection rules. Aside from the resonance condition $m = q+s$ owing to the separate orthogonality of the exponentials in eq. (25) these arise from properties of the Legendre functions [17]. Among the $\mathcal{O}({n_{max}}^6)$ coupling coefficients only $\mathcal{O}({n_{max}}^5)$ nonzero ones remain. For evaluation of the coupling integral see [18].

For convenience of notation we now switch to the set of real modes

$$\begin{aligned}&\{f_\alpha; \alpha = 1, \cdots, N\}\\ &= \left\{P_n^0, \sqrt{2}\,P_n^m \cos(m\lambda), \sqrt{2}\,P_n^m \sin(m\lambda); n = 1, \cdots, n_{max}; m = 1, \cdots, n; n+m \ \text{ odd}\right\}\end{aligned}$$

satisfying

$$< f_\alpha, f_\beta > = \delta_{\alpha\beta} \tag{29}$$

and

$$\Delta f_\alpha = -n(n+1) f_\alpha\,. \tag{30}$$

In this study the expansion is truncated at wavenumber $n_{\max} = 21$. This yields a linear subspace $\mathcal{H}$ spanned by $N = 231$ real modes ($N = \frac{n_{\max}(n_{\max}+1)}{2}$). The coefficient κ_2 of the scale selective diffusion term is set to a value representing a damping time scale of 3 days in the smallest scale (wavenumber 21). The diffusion term accounts for the neglected interactions with the unresolved modes. Their mean influence on the resolved modes can be parametrized by a linear damping. The external forcing is specified from a 500hPa streamfunction analysis data set in a way that the system has a realistic mean state and a variance pattern similar to that of 10 days running mean streamfunction fields. See [7] for the detailed procedure.

Moreover it is convenient to separate the flow Ψ into the time-independent mean flow $\overline{\Psi}$ and the anomalies Ψ'. The expansion (19) then reads

$$\Psi(\lambda, \mu, t) = \overline{\Psi}(\lambda, \mu) + \sum_{\alpha=1}^{N} \Psi'_\alpha(t) f_\alpha(\lambda, \mu)\,. \tag{31}$$

The dynamic equations for the Ψ'_α can be summarized to :

$$\dot{\Psi}'_\alpha = \frac{1}{2} \sum_{\beta,\gamma=1}^{N} A^{\text{sh}}_{\alpha\beta\gamma} \Psi'_\beta \Psi'_\gamma + \sum_{\beta=1}^{N} B^{\text{sh}}_{\alpha\beta} \Psi'_\beta + C^{\text{sh}}_\alpha \tag{32}$$

Eq. (32) forms a forced, dissipative system with quadratic nonlinearity. The quadratic term represents nonlinear wave-wave interactions; the linear term includes mean-wave interactions, the Coriolis effect, the topography and the friction terms; the forcing term is formed by the external forcing and the time-independent terms arising from the separation into mean flow and deviations from it. The superscript sh signifies that the quantities refer to spherical harmonics. The tensors of coefficients $A^{\text{sh}}, B^{\text{sh}}$ and C^{sh} can be derived easily from those occurring in eq. (24). The system of equations is integrated in time using the transform method [19] involving only $\mathcal{O}(N^{\frac{3}{2}})$ operations for each evaluation of the right side and a standard ODE integrator of high order.

The finite subspace $\mathcal{H}$ spanned by the 231 Fourier modes is of course not an inertial manifold of eq. (13) in a rigorous mathematical sense but it turns out to be sufficient to capture the long-term behaviour as far as first and second moments (e. g. energy spectra) are concerned. The system exhibits chaotic behaviour (continous spectra, positive Lyapunov exponents). It reproduces some essential features of atmospheric behaviour quite well (red spectrum, preferred flow patterns). Therefore the system of 231 ordinary differential equations can be regarded as a rough model of the large-scale atmospheric circulation. It will be the complex system we start out from to derive reduced models.

From now on all quantities and operators are replaced by their projection onto $\mathcal{H}$. Hence $\Psi, \overline{\Psi}, \Psi', \dot{\Psi}, \tilde{\Psi}, f$ and h have to be read as vectors of spherical harmonics coefficients in N-dimensional space; Δ as a diagonal $(N \times N)$-matrix with the eigenvalues of eq. (30) on its diagonal and $\mathcal{J}$ as a nonlinear map from $\mathcal{H} \times \mathcal{H}$ into $\mathcal{H}$. The scalar product $<\cdots,\cdots>$ corresponds to the canonical scalar product in $\mathcal{R}^N$ because of eq. (29).

4.2 Principal Interaction Patterns

Now we consider an L-dimensional subspace $\mathcal{P}$ in $\mathcal{H}$ spanned by the Principal Interaction Patterns. The streamfunction anomalies are expanded into a series of PIPs :

$$\Psi = \overline{\Psi} + \sum_{i=1}^{L} z_i \, p_i \tag{33}$$

The vector of expansion coefficients is

$$z = P^{+} \Psi' \, . \tag{34}$$

A reduced model is then defined by a projection of the terms in eq.(13) onto PIP-space:

$$\begin{aligned} \mathcal{T}\dot{\Psi} \; + \; & \mathcal{T}\Delta^{-1}\mathcal{J}\left[\overline{\Psi} + \mathcal{T}\Psi', \Delta\left(\overline{\Psi} + \mathcal{T}\Psi'\right) + f + h\right] \\ = \; & -\kappa_1 \mathcal{T}\left(\overline{\Psi} + \mathcal{T}\Psi'\right) - \kappa_2 \mathcal{T}\Delta^3\left(\overline{\Psi} + \mathcal{T}\Psi'\right) + \mathcal{T}\tilde{\Psi} \end{aligned} \tag{35}$$

$\mathcal{T}$ signifies the projection operator onto PIP-space, a linear map from $\mathcal{H}$ into $\mathcal{H}$ given by the $(N \times N)$-matrix

$$\mathcal{T} = P P^{+} \, . \tag{36}$$

This yields a system of ordinary differential equations for the PIP-amplitudes z of the form

$$\dot{z}_i^{\mathrm{PIP}} = G_i = \frac{1}{2} \sum_{j,k=1}^{L} A_{ijk} z_j z_k + \sum_{j=1}^{L} B_{ij} z_j + C_i \tag{37}$$

where the coefficients are given by

$$A_{ijk} = - <p_i^*, M\Delta^{-1}\left[\mathcal{J}(p_j, \Delta p_k) + \mathcal{J}(p_k, \Delta p_j)\right]> \tag{38}$$

$$B_{ij} = - <p_i^*, M\left(\Delta^{-1}\left[\mathcal{J}(\overline{\Psi}, \Delta p_j) + \mathcal{J}(p_j, \Delta\overline{\Psi} + f + h)\right] + \kappa_1 p_j + \kappa_2 \Delta^3 p_j\right)> \tag{39}$$

$$C_i = <p_i^*, M\left(\tilde{\Psi} - \Delta^{-1}\mathcal{J}(\overline{\Psi}, \Delta\overline{\Psi} + f + h) - \kappa_1\overline{\Psi} - \kappa_2\Delta^3\overline{\Psi}\right)> \, . \tag{40}$$

$\dot{z}^{\mathrm{PIP}}$ denotes the tendencies of the PIP-amplitudes as given by the truncated model in contradistinction from the exact tendencies $\dot{z} = P^{+}\dot{\Psi}$. This kind of truncation is

equivalent to a projection of the tensors of interaction coefficients of the full system :

$$A_{ijk} = \sum_{\alpha,\beta,\gamma=1}^{N} P^{+}_{i\alpha} P_{\beta j} P_{\gamma k} A^{\mathrm{sh}}_{\alpha\beta\gamma} \tag{41}$$

$$B_{ij} = \sum_{\alpha,\beta=1}^{N} P^{+}_{i\alpha} P_{\beta j} B^{\mathrm{sh}}_{\alpha\beta} \tag{42}$$

$$C_i = \sum_{\alpha=1}^{N} P^{+}_{i\alpha} C^{\mathrm{sh}}_{\alpha} \tag{43}$$

The elements of the tensors A, B and C form the set of parameters σ. Hence the parameters in this case are connected to the patterns rather than determined independently from them.

In the present calculations three different metrics M for defining the projection are considered which have particular physical meaning : $M_1 = 1$, the squared anomaly streamfunction metric; $M_2 = -\Delta$, the turbulent kinetic energy metric; and $M_3 = \Delta^2$, the turbulent enstrophy and squared anomaly vorticity metric.

Note that eqs. (33)-(43) are completely general; they hold for any L-dimensional subspace $\mathcal{P} \subseteq \mathcal{H}$ spanned by L arbitrary linearly independent modes. Especially, if the patterns are chosen as spherical harmonics and M_1 is chosen as metric one returns to the corresponding coupling coefficients of the full system in eq. (32).

A special choice of PIPs are the EOFs. In the following subsection the definition and the main properties of EOFs are reviewed briefly.

4.3 Empirical Orthogonal Functions

Starting out from an N-dimensional state vector $\Phi(t)$ one may ask for an expansion using only S spatial modes ($S < N$) which converges optimally fast in the sense that the mean squared error in the representation of Φ

$$\epsilon_S = \overline{\left(\Phi - \sum_{\alpha=1}^{S} \hat{\Phi}_\alpha e_\alpha\right)^t \bar{M} \left(\Phi - \sum_{\alpha=1}^{S} \hat{\Phi}_\alpha e_\alpha\right)} \tag{44}$$

with

$$\hat{\Phi}_\alpha = e^t_\alpha \bar{M} \Phi \tag{45}$$

be minimized subject to

$$e^t_\alpha \bar{M} e_\beta = \delta_{\alpha\beta} \qquad \alpha, \beta = 1, \cdots, S\,. \tag{46}$$

$\bar{M}$ may be an arbitrary symmetric, positive definite metric. It is well known that the solution to this minimization problem is given by the eigenvectors corresponding to the S largest eigenvalues of the eigenvalue problem

$$\Gamma \bar{M} e_\alpha = \lambda^{\mathrm{eof}}_\alpha e_\alpha \tag{47}$$

Γ being the matrix of second moments of Φ :

$$\Gamma_{\alpha\beta} = \overline{\Phi_\alpha \Phi_\beta} \qquad \alpha, \beta = 1, \cdots, N \tag{48}$$

The matrix $\Gamma\bar{M}$ as a product of symmetric, positive definite matrices can be diagonalized in a real basis and has only real and positive eigenvalues. The amplitudes of the EOFs $\hat{\Phi}_\alpha$ are pairwise uncorrelated and the second moment of each is given by the corresponding eigenvalue :

$$\overline{\hat{\Phi}_\alpha \hat{\Phi}_\beta} = \delta_{\alpha\beta}\lambda_\alpha^{\text{eof}} \tag{49}$$

The mean squared error is then given by

$$\epsilon_S = \sum_{\alpha=S+1}^{N} \lambda_\alpha^{\text{eof}} \tag{50}$$

EOFs may be calculated either from the full state vector Φ or only from the anomalies $\Phi' = \Phi - \overline{\Phi}$. See [20] for an extensive overview on the mathematical properties of EOF-analysis.

Note that the EOFs are only optimal for capturing as much variance as possible with a given number of modes. To construct a reduced system it is necessary to describe the time evolution of the modes chosen as basis functions. For this purpose one has to model not only the state itself, but also the terms occurring in the dynamical equation governing the time evolution, e. g. the spatial derivatives (cf. [8]). This is not implied with EOFs. The optimality criterion does not refer to dynamics at all. Nevertheless the EOFs may be regarded as an attractive candidate for a set of basis functions in a reduced model since they already take into account the characteristics of the system under consideration to a large extent (the structure of the second moments) compared to eigenfunctions of a linear differential operator, here spherical harmonics, which are completely general.

4.4 Conserved quantities of truncated models

In view of the conserved integral quantities of eq. (13) one may ask if this conservation properties are adopted by truncated systems. The corresponding projected quantities in L-dimensional PIP-space are

$$E_{\text{kin}}^{\text{pip}} = -\frac{1}{2} < \overline{\Psi} + \mathcal{T}\Psi', \Delta\left(\overline{\Psi} + \mathcal{T}\Psi'\right) > \tag{51}$$

and

$$ENS^{\text{pip}} = \frac{1}{2} < \Delta\left(\overline{\Psi} + \mathcal{T}\Psi'\right), \Delta\left(\overline{\Psi} + \mathcal{T}\Psi'\right) > . \tag{52}$$

If the full streamfunction is expanded into a series of PIPs the following statements hold: For reduced systems based on spherical harmonics it can be shown that the terms arising from the truncated Jacobian (nonlinear interactions, Coriolis and topography term) conserve both kinetic energy and (except for the topography) enstrophy for all three metrics considered (especially the full system of eq. (32) does). As a consequence the flow in phase space associated with the nonlinear terms is divergence-free (Liouvillian property). This does not hold in the case of general patterns. This difference is due to the fact that in case of spherical harmonics the projection operator $\mathcal{T}$ and Δ commute because of eq. (30), whereas in the general case they do not. Then the conservation properties depend on the metric M used in the projection procedure. If the kinetic energy metric M_2 is used the quadratic terms, the Coriolis and the topography terms of

the PIP-model conserve the truncated kinetic energy $E_{\rm kin}^{\rm pip}$, if the enstrophy metric M_3 is used enstrophy is conserved by the nonlinear interactions and the Coriolis term; in the case of the norm streamfunction metric M_1 no conserved quantity exists. It is in general not possible to conserve both kinetic energy and enstrophy by the quadratic terms in a reduced model defined according to the formulae (37)-(40). Also the divergence of the nonlinear terms generally does not vanish. Actually there are alternative formulations of truncated models which allow for conservation of both integral quantities (see [7]) but these are unfavourable for other reasons and are not considered here. If the mean state is prescribed and only the streamfunction anomalies are expanded into a series of PIPs (as is done in this study; cf. eq. (33)) the statements mentioned above hold for the turbulent kinetic energy

$$E_{\rm kin}^{\prime\,\rm pip} = -\frac{1}{2} <\mathcal{T}\Psi', \Delta\mathcal{T}\Psi'>= -\frac{1}{2} z^t P^t \Delta P z \tag{53}$$

and the turbulent enstrophy

$$ENS^{\prime\,\rm pip} = \frac{1}{2} <\Delta\mathcal{T}\Psi', \Delta\mathcal{T}\Psi'>= \frac{1}{2} z^t P^t \Delta^2 P z\,, \tag{54}$$

both projected onto PIP-space, instead of $E_{\rm kin}^{\rm pip}$ and $ENS^{\rm pip}$. Note that the existence of at least one conserved quantity for the quadratic interactions guarantees that the solutions of the reduced system are bounded for all times. The conservation statements can be proven quite easily with the help of eqs. (5) and (36) and the following identities valid for all $a, b \in \mathcal{H}$:

$$<a, \mathcal{J}(a,b)> = <b, \mathcal{J}(a,b)> = 0 \tag{55}$$

$$<a, \Delta b> = <\Delta a, b> \tag{56}$$

$$<a, \mathcal{J}(b,f)> = -<\mathcal{J}(a,f), b> \tag{57}$$

5 Determination of the optimal truncated system

We now seek a reduced system which is optimal in the sense of the variational principle expressed in eq. (10). Since for a given set of patterns the parameters are determined by the projection procedure the components of the patterns are the only independent variables and the problem is actually to identify an optimal L-dimensional linear subspace $\mathcal{P}$ in $\mathcal{H}$.

5.1 Uniqueness of the PIP-model

It is evident that the Principal Interaction Patterns are only determined to within a linear transformation. Consider an arbitrary regular linear transformation R in L-dimensional space and a matrix of patterns P. The transformed set of patterns is then $P' = PR$, the corresponding vector of expansion coefficients is $z' = R^{-1}z$. The interaction coefficients A, B and C are transformed according to the rules for tensors of third, second and first order, respectively :

$$A'_{ijk} = \sum_{m,p,q} R^{-1}_{im} R_{pj} R_{qk} A_{mpq} \tag{58}$$

$$B'_{ij} = \sum_{m,n} R^{-1}_{im} R_{nj} B_{mn} \tag{59}$$

$$C'_i = \sum_m R^{-1}_{im} C_m \tag{60}$$

The error function Q is invariant under this transformation : $Q(P') = Q(P)$

To eliminate this gauge freedom one has to refer to some normal form for the matrix of patterns. One possibility to do so is to impose the constraints that the patterns be orthogonal with respect to M, that their amplitudes be uncorrelated with the patterns ordered by descending mean squared amplitude and that the coefficients C_i be always positive :

$$p_i^t M p_j = \delta_{ij} \tag{61}$$

$$\overline{z_i z_j} = p_i^{*t} M \Gamma M p_j^* = \lambda_i^{\mathrm{pip}} \delta_{ij} \qquad \lambda_i^{\mathrm{pip}} > \lambda_{i+1}^{\mathrm{pip}} \tag{62}$$

$$C_i \geq 0 \tag{63}$$

Besides this gauge freedom the existence of several sets of patterns sharing the same value of the error function cannot be excluded rigorously since Q is highly nonlinear in P but generically does not occur.

5.2 Reduction of dimension using EOFs

The projection procedure is carried out in two steps. In order to reduce the number of variables in the minimization procedure the Principal Interaction Patterns and therewith also the adjoint patterns are assumed to lie in the S-dimensional subspace $\mathcal{E}$ spanned by the first S EOFs calculated from the streamfunction anomalies with respect to M ($\bar{M} = M; L \leq S \leq N; \mathcal{P} \subseteq \mathcal{E} \subseteq \mathcal{H}$) :

$$p_i = \sum_{\alpha=1}^{S} \hat{P}_{\alpha i}\, e_\alpha \qquad \text{or} \qquad P = E\hat{P} \tag{64}$$

E is the $(N \times S)$-matrix of the first S EOFs; $\hat{P}$ is the $(S \times L)$-matrix with the PIPs $\hat{p}$ expressed in terms of their EOF-coefficients as its column vectors. The EOFs are orthonormal with respect to M ($e_\alpha^t M e_\beta = \delta_{\alpha\beta}$). It is sufficient then to consider the projection of the system onto these S EOFs. Let $\hat{\Psi}$ and $\hat{\dot{\Psi}}$ be the vectors of EOF-coefficients of the streamfunction anomalies and their time derivatives, respectively :

$$\hat{\Psi} = E^t M \Psi' \tag{65}$$

$$\hat{\dot{\Psi}} = E^t M \dot{\Psi} \tag{66}$$

The vector of PIP-coefficients is then

$$z = \hat{P}^+ \hat{\Psi} \tag{67}$$

with

$$\hat{P}^+ = \hat{P}^{*t} = \left(\hat{P}^t \hat{P}\right)^{-1} \hat{P}^t\,, \tag{68}$$

$\hat{P}^*$ being the $(S \times L)$-matrix of adjoint patterns in the EOF-representation.

This restriction in the choice of the patterns is motivated as follows : First, it is simply a necessity to reduce the number of variables in the minimization procedure by restricting the choice of patterns somehow to stay within the limits of available computer power. Moreover the study of Selten [7] referring to the same fluid system and finding a reduced model based on 20 EOFs capable of both capturing the global behaviour of the system and predicting the flow for some time supports the expectation that the EOFs actually are already a good approximation to the optimal dynamical modes and that the PIPs will have largest contributions from leading EOFs.

5.3 The variational principle

The variational principle now reads :

$$\begin{aligned} Q(\hat{P}) &= \overline{(\dot{z}^{\mathrm{PIP}} - \dot{z})^t \tilde{M} (\dot{z}^{\mathrm{PIP}} - \dot{z})} \\ &= \overline{\left[G\left(z(\hat{P}),\sigma(\hat{P})\right) - \hat{P}^+\dot{\hat{\Psi}}\right]^t \tilde{M} \left[G\left(z(\hat{P}),\sigma(\hat{P})\right) - \hat{P}^+\dot{\hat{\Psi}}\right]} = \mathrm{Min.} \end{aligned} \tag{69}$$

subject to

$$\hat{p}_i^t \hat{p}_j = \delta_{ij} \tag{70}$$

$$\overline{z_i z_j} = \hat{p}_i^{*t} \hat{\Gamma} \hat{p}_j^* = \delta_{ij} \lambda_i^{\mathrm{pip}} \qquad \lambda_i^{\mathrm{pip}} > \lambda_{i+1}^{\mathrm{pip}} \tag{71}$$

$$C_i \geq 0 \tag{72}$$

with

$$\tilde{M} = \hat{P}^t \hat{P} (\hat{P}^t \hat{\Pi} \hat{P})^{-1} \hat{P}^t \hat{P} \tag{73}$$

$$\hat{\Gamma} = E^t M \Gamma M E \tag{74}$$

$$\hat{\Pi} = E^t M \Pi M E \tag{75}$$

For the patterns spanning the S-dimensional subspace $\mathcal{E}$ one has the same gauge freedom as with the PIPs. For numerical reasons it is convenient actually not to work with the EOFs themselves but with a set of patterns E' which is related to the EOFs by an orthonormal linear transformation U in S-dimensional space ($E = E'U$) chosen in a way that $\hat{\Pi}' = U^t E'^t M \Pi M E' U$ becomes diagonal while still preserving the orthonormality of the patterns ($e_\alpha'^t M e'_\beta = \delta_{\alpha\beta}$).

See the appendix for details on the calculation techniques of the minimization procedure.

5.4 Ill-conditioning and stability of the pattern identification

When dealing with chaotic systems one may ask about the stability of the pattern identification from a finite time series. There are two potential sources of errors in the algorithm : First, the EOFs of the system are not exactly known but only estimated from a finite sample of data, secondly, the nonlinear minimization to determine the PIPs also refers only to a finite sample of data. The latter one causes difficulties especially in the case that the minimization problem is ill-posed, as one expects for chaotic systems.

In the following the sampling problem in the estimation of EOFs is sketched briefly. The discussion is restricted to the case $\bar{M} = 1$ (symmetric eigenvalue problem). The

general case of eq. (47) is related to a symmetric eigenvalue problem by a similarity transformation with the matrix $\bar{M}^{\frac{1}{2}}$ and can be treated in an anagolous manner. Let Γ be the exact covariance matrix of the system, $\tilde{\Gamma}$ a symmetric matrix of perturbations due to the sampling error and ϵ a small parameter. Then the perturbed eigenvalue problem is :

$$\left(\Gamma + \epsilon\tilde{\Gamma}\right)(e_\alpha + \tilde{e}_\alpha) = \left(\lambda_\alpha^{\text{eof}} + \tilde{\lambda}_\alpha^{\text{eof}}\right)(e_\alpha + \tilde{e}_\alpha) \tag{76}$$

Classical perturbation theory for symmetric linear operators in the generic non-degenerated case yields for the errors in the eigenfunctions to first order :

$$\tilde{e}_\alpha = \epsilon \sum_{\beta \neq \alpha} \frac{e_\alpha^t \tilde{\Gamma} e_\beta}{\lambda_\alpha^{\text{eof}} - \lambda_\beta^{\text{eof}}} e_\beta + \mathcal{O}(\epsilon^2) \tag{77}$$

Hence mixing occurs mainly among neighbouring EOFs. The estimation of the subspace of the first S EOFs is thus much more stable than the estimation of individual higher modes. Suppose a relevant subspace of S EOFs contributing to the PIPs within a certain accuracy. Then this subspace can be assumed to be covered independent of the data sample by working with S' EOFs, S' slightly larger than S. For a more detailed discussion of the sampling problem see North et. al. [21].

The minimization problem turns out to be ill-posed. This difficulty may be coped with by applying an appropriate regularization procedure in analogy to singular value decomposition in the case of ill-conditioned linear least-squares problems. An adequate quadratic regularization term Q_{reg} to be added to the error function Q with some weighting is in the present context :

$$Q_{\text{reg}} = \frac{1}{2}\left[1 - \frac{1}{L}\sum_{\alpha=1}^{L}\sum_{i=1}^{L}\hat{P}_{\alpha i}^2 + \frac{1}{L}\sum_{\alpha=L+1}^{S}\sum_{i=1}^{L}\hat{P}_{\alpha i}^2\right] \tag{78}$$

It measures the deviation of the PIP-space from the subspace of the first L EOFs and takes values between 0 and 1 for sets of patterns satisfying the constraint of eq. (70). If the PIP-space is identical with the space of the L leading EOFs then $Q_{\text{reg}} = 0$; if it is orthogonal to the L leading EOFs then $Q_{\text{reg}} = 1$. Consider a convex linear combination of Q and Q_{reg} :

$$Q' = \eta Q + (1 - \eta)Q_{\text{reg}} \qquad 0 \leq \eta \leq 1 \tag{79}$$

In the case $\eta = 0$ the solution to the minimization problem is then given by the EOF-model with L modes, which can be stably determined from a finite sample if L is not too large. With increasing value of η more and more information from the variational principle is included. Using several independent data samples the maximum value of η for which the pattern identification is stable can be determined. Hence the EOF-model serves as a kind of minimum standard; an improvement of the patterns, as far as possible on the basis of the available data, is made in a controlable way.

An additional problem is the possible occurence of several local minima. Because of the nonlinearity of Q there are neither rigorous statements on the existence of local minima nor systematic ways to avoid them in the numerical minimization procedure. Nevertheless with the system considered in this study always only one minimum was found in several minimization procedures starting from different initial pattern sets.

6 Results and Discussion

The EOFs of the system have been estimated from a data sample of 50000 points. Fig. 1 gives an overview on the distribution of variance in the system with respect to the three different metrics.

Minimizations of the error function have been carried out for increasing numbers of Principal Interaction Patterns and different numbers of retained EOFs using the three different metrics. They are based on a data sample of 10000 points; i. e. the time average in the variational principle is taken as a time average over this data set. In all cases the minimization starts out from the first L EOFs taken as a first guess for the patterns (except for some control runs to check the independence upon the initial pattern set). Best results were obtained using the kinetic energy metric. Hence the study focuses mainly on this case. It turned out to be sufficient to search for the PIPs in a subspace $\mathcal{E}$ of 60 EOFs; no substantial improvement could be obtained by inclusion of higher modes.

6.1 Long-term behaviour

12 patterns turned out to be the minimum number of degrees of freedom to reproduce the first and second moments in PIP-space quite faithfully. The mean state is reproduced almost perfectly. Because of eqs.(33) and (34) the mean PIP-amplitudes in the full system are zero. A statistically significant deviation of the mean PIP-amplitudes obtained from a long-term integration with the reduced model from zero can be detected, but it is very small. The relative root squared error in the mean state $\sqrt{\frac{<P\bar{z},P\bar{z}>}{<\Psi,\Psi>}}$ is 0.02, the error in the kinetic energy of the mean state is less than 0.3%.

Long-term integrations of the reduced models show that they tend to have systematically too much variance (and also too much energy and enstrophy). This is due to the fact that the horizontal diffusion term which removes energy from the tail of the spectrum is not captured very well by the PIP-model since it affects mainly the modes of high wavenumbers whereas the PIPs are concentrated on the long and medium waves (large-scale patterns). This difficulty may be solved by introducing an additional linear damping in the evolution equations for the PIP-amplitudes to parametrize the mean effect of the unresolved modes on the resolved PIP-modes in analogy to the additional diffusion term incorporated in the spectral model. In the present framework this can be done by calculating the elements of B as independent variables according to the variational principle simultaneously with the patterns instead of determining them via eq. (39). Fig. 2 shows the energy spectrum obtained from a long-term integration of a PIP-model using 12 modes without additional damping, Fig. 3 with additional damping. Both figures refer to the pattern set obtained from the minimization with additional damping. The integration time is taken so long that the errors in the estimation of the second moments are actually negligible. The additional linear damping yields a considerable improvement. The total mean turbulent kinetic energy in PIP-space is now 5% too small; without the damping it is 26% too large. From now on only reduced models with additional damping are considered. We now look at the full second-order statistics in PIP-space. Fig. 4 illustrates the mean squared amplitude of the PIP-modes obtained from the reduced model and from the full model. Except for the sixth pattern the accordance is very good. Table 1 gives the correlation matrix of the PIP-amplitudes

in the simulation with the reduced model. The standard errors are of the order 10^{-3}. The PIPs are rotated in a way that their amplitudes are uncorrelated in the data of the full system (cf. section 5.1, eq. (62)). Hence the correlation matrix would be the unity matrix in the ideal case. The deviations from zero in the present values are statistically highly significant except for the values indicated as zero. Nevertheless the majority of the values is close to zero. The PIP-model is able to reproduce the second-moment structure in PIP-space quite well.

Fig. 5 shows the energy spectrum obtained from a simulation using 17 EOFs. With truncated models based on EOFs it was not possible to reproduce the energy spectrum with less than 17 modes.

To compare the 12-dimensional PIP-space with the space of the leading 12 EOFs the squared normalized projection $\sum_i < e_\alpha, Mp_i >^2 = \sum_i \hat{P}^2_{\alpha i}$ is given in Fig. 6 for each EOF e_α. The PIP-space is dominated by the leading 12 EOFs but also contains considerable contributions from higher EOFs. The sharp decrease between the 12th and 13th EOF is due to the particular regularization procedure. If the EOFs in eq.(78) would be e. g. weighted by their variance the decrease would be smoother, but the regularization is then less efficient.

The PIP-space spanned by the 12 modes captures 59.4% of the total mean turbulent kinetic energy; the first 12 EOFs contain 69.0%, the first 17 EOFs 76.4%. But the PIP-model still reproduces the essentials of the large-scale pattern evolution.

If the turbulent enstrophy metric $M_3 = \Delta^2$ is used in the projection the same minimum numbers of modes to reproduce the mean and the covariance structure of the amplitudes (12 PIPs, 17 EOFs) were found. But the fraction of energy and enstrophy captured by these 12 PIPs is smaller than in the case of $M_2 = -\Delta$. With the norm anomaly streamfunction metric $M_1 = 1$ the minimum reduced model has to include 15 patterns. This higher number may be due to the fact that the nonlinear terms in this case have no conserved quantity.

6.2 Local properties

Fig. 7a shows the correlation between the tendencies of the PIP-amplitudes given by the truncated model and those given by the full model separately for each pattern :

$$\mathrm{cor}_i = \frac{\mathrm{Cov}(\dot{z}_i^{\mathrm{PIP}}, \dot{z}_i)}{\sqrt{\mathrm{Var}(\dot{z}_i^{\mathrm{PIP}})}\sqrt{\mathrm{Var}(\dot{z}_i)}} \qquad i = 1, \cdots, L \tag{80}$$

Fig. 7b gives the explained tendency variance for each pattern defined by :

$$s_i = 1 - \frac{\mathrm{Var}(\dot{z}_i^{\mathrm{PIP}} - \dot{z}_i)}{\mathrm{Var}(\dot{z}_i)} \qquad i = 1, \cdots, L \tag{81}$$

The quantities are estimated from a data sample of 50000 points different from the sample used for the minimization. The standard errors of the estimates of cor_i and s_i are of the order 10^{-3} and are therefore not indicated in detail. For all PIP-modes a very large part of the tendency variance is explained by the reduced model.

The corresponding values for the first 12 EOFs are in Fig. 8a/b. The PIP-model provides a considerable improvement on the EOF-model; even the tendencies of the EOFs are captured better by the PIP-model than by the EOF-model. About 17 EOFs are necessary to describe the tendencies of the first 12 EOFs as well as with 12 PIPs.

6.3 Prediction experiments

Now the ability of the truncated model to predict the time evolution of the PIP-amplitudes for a finite time is investigated. Starting out from an initial anomaly field $\Psi'(0)$ the PIP-model is integrated in time with the initial condition $z(0) = P^+\Psi'(0)$. The quality of the forecasts as a function of the prediction time τ is measured by the mean anomaly correlation

$$\{\mathrm{Acor}(\tau)\} = \left\{ \frac{<\Psi'^{\mathrm{pip}}(\tau), \Psi'^{\mathrm{pred}}(\tau)>}{\sqrt{<\Psi'^{\mathrm{pip}}(\tau), \Psi'^{\mathrm{pip}}(\tau)>}\sqrt{<\Psi'^{\mathrm{pred}}(\tau), \Psi'^{\mathrm{pred}}(\tau)>}} \right\} \tag{82}$$

and the relative root mean squared error

$$\mathrm{rrmse}(\tau) = \sqrt{\frac{\{<\Psi'^{\mathrm{pip}}(\tau) - \Psi'^{\mathrm{pred}}(\tau), \Psi'^{\mathrm{pip}}(\tau) - \Psi'^{\mathrm{pred}}(\tau)>\}}{\{<\Psi'^{\mathrm{pip}}(\tau), \Psi'^{\mathrm{pip}}(\tau)>\}}}. \tag{83}$$

$\Psi'^{\mathrm{pip}}(\tau) = PP^+\Psi'(\tau)$ is the anomaly field at time τ given by the full model projected onto PIP-space; $\Psi'^{\mathrm{pred}}(\tau) = Pz(\tau)$ is the field predicted by the PIP-model. The braces denote an average over the ensemble of forecasts, here 2000 uncorrelated forecasts. The forecast periods are different from the data sample used to determine the PIPs. The persistence forecast $\Psi'^{\mathrm{pers}}(\tau) = \Psi'^{\mathrm{pip}}(0)$ simply reflecting the autocorrelation of the PIP-amplitudes is considered as a trivial control forecast. Note that the integration of the full model starts from the full initial condition $\Psi'(0)$. Figs. 9a and 9b show the results. The PIP-forecasts using 12 patterns have considerable skill.

The errors in the prediction experiments consist of two parts : The first part comes from the truncation error of the reduced system. Moreover the projection onto the PIPs causes an error in the initial condition which leads to prediction errors due to the inherent instability present in the full system. To investigate the influence of the truncation error alone further prediction experiments have been performed starting from initial conditions $PP^+\Psi'(0)$ lying in PIP-space instead of $\Psi'(0)$. Hence now the PIP-model and the reference integration with the full model start from the same initial condition. The forecast skill is now much better (Fig. 10 a/b). This indicates that a large part of the errors in Figs. 9a and 9b is due to the error in the initial condition.

Last the ability of the reduced models to predict the time evolution of the most energetic components is investigated. Figs. 11a and 11b refer to the same prediction experiments as Fig. 9a/b, but now the skill concerning the amplitudes of the first 12 EOFs instead of the PIPs is evaluated. The PIP-model starts with an error at the beginning since the EOFs are not fully contained in PIP-space. But after some time the predictions with the PIP-model are better than those with the EOF-model because the dynamics are captured better by the PIP-model.

7 Conclusions

An algorithm for constructing optimal low-dimensional models of complex dynamical systems has been described. An optimal linear subspace spanned by a few characteristic spatial patterns and the coefficients of a dynamical system describing the time evolution of these modes are determined simultaneously according to a variational principle. The

method involves higher-order correlation tensors of the variables and their time derivatives and leads to a nonlinear minimization problem in contrast to e. g. EOF-analysis which is based on second-order statistics and leads to an eigenvalue problem. In an application to a two-dimensional fluid system the EOFs turn out to be already a rather good approximation to the optimal modes, but the PIPs provide a considerable improvement, a PIP-model with 12 modes being approximately as good as an EOF-model with 17 patterns as to both global behaviour monitored by second-order statistics and short time prediction skill.

Acknowledgements

Part of this work was prepared during a visit to the Royal Netherlands Meteorological Institute. I would like to thank F. Selten for providing the computer code of the barotropic spectral model and for helpful discussions.

References

[1] **L. Sirovich,** Chaotic dynamics of coherent structures, Physica D 37, 126 (1989)

[2] **L. Sirovich,** Turbulence and the dynamics of coherent structures, Parts I-III, Q. Appl. Math. XLV, 561, (1987)

[3] **L. Sirovich, B. W. Knight and J. D. Rodriguez,** Optimal low-dimensional dynamical approximations, Q. Appl. Math. XLVIII, 535 (1990)

[4] **J. D. Rodriguez and L. Sirovich,** Low-dimensional dynamics for the complex Ginzburg-Landau equation, Physica D 43, 77 (1990)

[5] **N. Aubry, P. Holmes, J. L. Lumley and E. Stone,** The dynamics of coherent structures in the wall region of a turbulent boundary layer, J. Fluid Mech. 192, 115 (1988)

[6] **F. M. Selten,** Toward an Optimal Description of Atmospheric Flow, J. Atmos. Sci. 50, 861-877 (1993)

[7] **F. M. Selten,** An Efficient Description of the Dynamics of Barotropic Flow, J. Atmos. Sci. (in press)

[8] **M. Kirby,** Minimal dynamical systems from PDEs using Sobolev eigenfunctions, Physica D 57, 466-475 (1992)

[9] **C. Uhl, R. Friedrich, H. Haken,** Reconstruction of spatio-temporal signals of complex systems, Z. Phys. B 92, 211-219 (1993)

[10] **C. Uhl, R. Friedrich, H. Haken,** Analysis of spatio-temporal signals of complex systems, submitted to Phys. Rev. E

[11] **U. Achatz, G. Schmitz, K.-M. Greisiger,** Principal Interaction Patterns in Baroclinic Wave Life Cycles, J. Atmos. Sci. (in press)

[12] **K. Hasselmann,** PIPs and POPs: The Reduction of Complex Dynamical Systems Using Principal Interaction and Oscillation Patterns, J. Geophys. Res. 93, 11015-11021 (1988)

[13] **J. Pedlosky,** Geophysical Fluid Dynamics, Springer, New York, 2nd ed. , 710 pp. (1987)

[14] **M. Ghil, S. Childress,** Topics in Geophysical Fluid Dynamics : Atmospheric Dynamics, Dynamo Theory, and Climate Dynamics, Springer, New York, 485 pp. (1987)

[15] **J. R. Holton,** An Introduction to Dynamic Meteorology, Academic Press, 3rd ed. , 511 pp. (1992)

[16] **I. Silberman,** Planetary waves in the atmosphere, J. Meteor. 11, 27-34 (1954)

[17] **G. W. Platzman,** The spectral form of the vorticity equation, J. Meteor. 17, 635-644 (1960)

[18] **H. W. Ellsaesser,** Evaluation of spectral versus grid methods of hemispheric numerical weather prediction, J. Appl. Meteor. 5, 246-262 (1966)

[19] **S. A. Orszag,** Transform method for calculation of vector-coupled sums: Application to the spectral form of the vorticity equation, J. Atmos. Sci. 27, 890-895 (1970)

[20] **R. W. Preisendorfer,** Principal component analysis in meteorology and oceanography, Elsevier, Amsterdam, 401 pp. (1988)

[21] **G. R. North, T. L. Bell, R. F. Cahalan, F. J. Moeng,** Sampling Errors in the Estimation of Empirical Orthogonal Functions, Mon. Wea. Rev. 110, 699-706 (1982)

A Minimization of the error function

The error function can be expressed in terms of moments of the PIP-coefficients and their time derivatives. In the following greek indices always run from 1 to S, latin ones from 1 to L.

$$\begin{aligned} & Q\left(\hat{P}, A(\hat{P}), B(\hat{P}), C(\hat{P})\right) \\ = & \sum_{m,n} \tilde{M}_{mn} \left[\frac{1}{4} \sum_{i,j,k,l} A_{mij} A_{nkl} \overline{z_i z_j z_k z_l} + \sum_{i,j,k} A_{mij} B_{nk} \overline{z_i z_j z_k} \right. \\ & + \sum_{i,j} \left(A_{mij} C_n + B_{mi} B_{nj}\right) \overline{z_i z_j} + 2 \sum_i B_{mi} C_n \overline{z_i} + C_m C_n \\ & \left. + \overline{\dot{z}_m \dot{z}_n} - 2 C_m \overline{\dot{z}_n} - \sum_{i,j} A_{mij} \overline{\dot{z}_n z_i z_j} - 2 \sum_i B_{mi} \overline{\dot{z}_n z_i} \right] \end{aligned} \tag{84}$$

The variation of Q with respect to the patterns $\hat{p}_i$ and the parameters A, B and C yields:

$$\begin{aligned} \frac{\partial Q}{\partial \hat{P}_{\alpha q}} = & \sum_{m,n} \frac{\partial \tilde{M}_{mn}}{\partial \hat{P}_{\alpha q}} \left[\frac{1}{4} \sum_{i,j,k,l} A_{mij} A_{nkl} \overline{z_i z_j z_k z_l} + \sum_{i,j,k} A_{mij} B_{nk} \overline{z_i z_j z_k} \right. \\ & + \sum_{i,j} \left(A_{mij} C_n + B_{mi} B_{nj}\right) \overline{z_i z_j} + 2 \sum_i B_{mi} C_n \overline{z_i} + C_m C_n \\ & \left. + \overline{\dot{z}_m \dot{z}_n} - 2 C_m \overline{\dot{z}_n} - \sum_{i,j} A_{mij} \overline{\dot{z}_n z_i z_j} - 2 \sum_i B_{mi} \overline{\dot{z}_n z_i} \right] \\ & + \sum_{m,n} \tilde{M}_{mn} \left[\sum_{i,j,k,l} A_{mij} A_{nkl} \overline{z_i z_j z_k \frac{\partial z_l}{\partial \hat{P}_{\alpha q}}} \right. \\ & + \sum_{i,j,k} A_{mij} B_{nk} \left(2 \overline{z_j z_k \frac{\partial z_i}{\partial \hat{P}_{\alpha q}}} + \overline{z_i z_j \frac{\partial z_k}{\partial \hat{P}_{\alpha q}}} \right) \\ & + 2 \sum_{i,j} \left(A_{mij} C_n + B_{mi} B_{nj}\right) \overline{z_i \frac{\partial z_j}{\partial \hat{P}_{\alpha q}}} + 2 \sum_i B_{mi} C_n \overline{\frac{\partial z_i}{\partial \hat{P}_{\alpha q}}} \\ & + 2 \overline{\dot{z}_m \frac{\partial \dot{z}_n}{\partial \hat{P}_{\alpha q}}} - 2 \sum_i C_m \overline{\frac{\partial \dot{z}_n}{\partial \hat{P}_{\alpha q}}} - \sum_{i,j} A_{mij} \left(2 \overline{\dot{z}_n z_i \frac{\partial z_j}{\partial \hat{P}_{\alpha q}}} + \overline{z_i z_j \frac{\partial \dot{z}_n}{\partial \hat{P}_{\alpha q}}} \right) \\ & \left. - 2 \sum_i B_{mi} \left(\overline{\dot{z}_n \frac{\partial z_i}{\partial \hat{P}_{\alpha q}}} + \overline{z_i \frac{\partial \dot{z}_n}{\partial \hat{P}_{\alpha q}}} \right) \right] \end{aligned} \tag{85}$$

with

$$\begin{aligned} \frac{\partial \tilde{M}_{mn}}{\partial \hat{P}_{\alpha q}} = & \sum_{i,j} \left(V_{ij} \left[\left(\delta_{mq} \hat{P}_{\alpha i} + \delta_{iq} \hat{P}_{\alpha m}\right) D_{jn} + \left(\delta_{nq} \hat{P}_{\alpha j} + \delta_{jq} \hat{P}_{\alpha n}\right) D_{im} \right] \right. \\ & \left. - D_{im} D_{jn} \sum_k \hat{\Pi}_{\alpha\alpha} \hat{P}_{\alpha k} \left(V_{ik} V_{jq} + V_{iq} V_{jk}\right) \right) \end{aligned} \tag{86}$$

$$\frac{\partial z_i}{\partial \hat{P}_{\alpha q}} = D^{-1}_{iq} \left(\hat{\Psi}_\alpha - \sum_k \hat{P}_{\alpha k} z_k \right) - \hat{P}^{+}_{i\alpha} z_q \tag{87}$$

$$\frac{\partial \dot{z}_i}{\partial \hat{P}_{\alpha q}} = D^{-1}_{iq} \left(\dot{\hat{\Psi}}_\alpha - \sum_k \hat{P}_{\alpha k} \dot{z}_k \right) - \hat{P}^+_{i\alpha} \dot{z}_q \tag{88}$$

$$D = \hat{P}^t \hat{P} \tag{89}$$

$$V = (\hat{P}^t \hat{\Pi} \hat{P})^{-1} \tag{90}$$

Without loss of generality $\hat{\Pi}$ is assumed to be diagonal in formula (86) (cf. section 5.3).

$$\frac{\partial Q}{\partial A_{lpq}} = \sum_i \tilde{M}_{il} \left(\frac{1}{2} \sum_{j,k} A_{ijk} \overline{z_j z_k z_p z_q} + \sum_j B_{ij} \overline{z_j z_p z_q} + C_i \overline{z_p z_q} - \overline{\dot{z}_i z_p z_q} \right) \tag{91}$$

$$\frac{\partial Q}{\partial B_{pq}} = \sum_i \tilde{M}_{ip} \left(\sum_{j,k} A_{ijk} \overline{z_j z_k z_q} + 2 \sum_j B_{ij} \overline{z_j z_q} + 2 C_i \overline{z_q} - 2 \overline{\dot{z}_i z_q} \right) \tag{92}$$

$$\frac{\partial Q}{\partial C_l} = \sum_i \tilde{M}_{il} \left(\sum_{j,k} A_{ijk} \overline{z_j z_k} + 2 \sum_j B_{ij} \overline{z_j} + 2 C_i - 2 \overline{\dot{z}_i} \right) \tag{93}$$

The total derivative with respect to the patterns reads :

$$\frac{dQ}{d\hat{P}_{\alpha q}} = \frac{\partial Q}{\partial \hat{P}_{\alpha q}} + \sum_{i,j,k} \frac{\partial Q}{\partial A_{ijk}} \frac{\partial A_{ijk}}{\partial \hat{P}_{\alpha q}} + \sum_{i,j} \frac{\partial Q}{\partial B_{ij}} \frac{\partial B_{ij}}{\partial \hat{P}_{\alpha q}} + \sum_i \frac{\partial Q}{\partial C_i} \frac{\partial C_i}{\partial \hat{P}_{\alpha q}} \tag{94}$$

The nonlinear minimization is performed using a standard Quasi-Newton method with BFGS-update applied to an augmented Lagrangian function treating the constraints with Lagrangian multipliers.

B Calculation of interaction coefficients

The computational effort to determine the interaction coefficients is dominated by the calculation of the Jacobian terms in eqs. (38)-(40). There are basically two possibilities to evaluate them. On the one hand one can calculate the Jacobians in the full phase space of spherical harmonics using the transform method. On the other hand it is possible to consider the Jacobians only in the subspace $\mathcal{E}$ of retained EOFs and then to proceed as follows. The tensors of coefficients $A^{\text{eof}}, B^{\text{eof}}$ and C^{eof} of the reduced model using the leading S EOFs as basis functions ($p_i = e_i, L = S$) are calculated once explicitly according to formulae (38)-(40) using the transform method :

$$A^{\text{eof}}_{\alpha\beta\gamma} = - < e_\alpha, M \Delta^{-1} [\mathcal{J}(e_\beta, \Delta e_\gamma) + \mathcal{J}(e_\gamma, \Delta e_\beta)] > \tag{95}$$

$$B^{\text{eof}}_{\alpha\beta} = - < e_\alpha, M \left(\Delta^{-1} \left[\mathcal{J}(\overline{\Psi}, \Delta e_\beta) + \mathcal{J}(e_\beta, \Delta \overline{\Psi} + f + h) \right] + \kappa_1 e_\beta + \kappa_2 \Delta^3 e_\beta \right) > \tag{96}$$

$$C^{\text{eof}}_\alpha = < e_\alpha, M \left(\tilde{\Psi} - \Delta^{-1} \mathcal{J}(\overline{\Psi}, \Delta \overline{\Psi} + f + h) - \kappa_1 \overline{\Psi} - \kappa_2 \Delta^3 \overline{\Psi} \right) > . \tag{97}$$

Here $e^*_\alpha = e_\alpha$ holds because of $e^t_\alpha M e_\beta = \delta_{\alpha\beta}$. In the actual calculations the rotated patterns e'_α introduced in section 5.3 are used instead of e_α, but the primes are dropped

now for convenience of notation. The coefficients of the PIP-model are then calculated by direct summation in the S-dimensional EOF-space using the identities

$$A_{ijk} = \sum_{\alpha,\beta,\gamma=1}^{S} \hat{P}^{+}_{i\alpha}\hat{P}_{\beta j}\hat{P}_{\gamma k}A^{\mathrm{eof}}_{\alpha\beta\gamma} \tag{98}$$

$$B_{ij} = \sum_{\alpha,\beta=1}^{S} \hat{P}^{+}_{i\alpha}\hat{P}_{\beta j}B^{\mathrm{eof}}_{\alpha\beta} \tag{99}$$

$$C_i = \sum_{\alpha=1}^{S} \hat{P}^{+}_{i\alpha}C^{\mathrm{eof}}_{\alpha} \tag{100}$$

The former method involves $\mathcal{O}(N^{\frac{3}{2}})$ operations for each Jacobian term, the latter one $\mathcal{O}(S^3)$ operations. Moreover the calculation in EOF-space requires storage of the $\mathcal{O}(S^3)$ interaction coefficients of the EOF-model. Hence the former method is preferable for large S, the latter one for small S. The turning point is about $S \approx 40$.

If the matrix B of linear interaction coefficients is determined from the variational principle rather than from the dynamic equation one has to solve a positive definite system of L^2 linear equations resulting from $\frac{\partial Q}{\partial B_{pq}} = 0$. In this equations the metric can be removed; the system then takes a block-diagonal structure and each row of B can be obtained separately from a positive definite linear system of dimension L :

$$\sum_j X_{sj}B_{ij} = y^i_s \tag{101}$$

with

$$\begin{aligned} X_{sj} &= \overline{z_s z_j} \\ y^i_s &= \overline{\dot{z}_i z_s} - \frac{1}{2}\sum_{j,k} A_{ijk}\,\overline{z_j z_k z_s} - C_i\,\overline{z_s} \end{aligned} \tag{102}$$

Note that the system matrix X is independent of i. Hence its Cholesky decomposition has to be computed only once for a given set of patterns; then all elements of B are obtained by backsubstitution.

C Derivative of interaction coefficients

The first order variation of the coefficients of the PIP-model with respect to the patterns yields :

$$\begin{aligned} \frac{\partial A_{ijk}}{\partial \hat{P}_{\alpha q}} &= -<\frac{\partial p^*_i}{\partial \hat{P}_{\alpha q}}, M\Delta^{-1}\left[\mathcal{J}(p_j,\Delta p_k)+\mathcal{J}(p_k,\Delta p_j)\right]> \\ &\quad -\delta_{jq}<p^*_i, M\Delta^{-1}\left[\mathcal{J}(e_\alpha,\Delta p_k)+\mathcal{J}(p_k,\Delta e_\alpha)\right]> \\ &\quad -\delta_{kq}<p^*_i, M\Delta^{-1}\left[\mathcal{J}(e_\alpha,\Delta p_j)+\mathcal{J}(p_j,\Delta e_\alpha)\right]> \\ &= D^{-1}_{iq}\left(\Lambda_{\alpha jk} - \sum_l \hat{P}_{\alpha l}A_{ljk}\right) - \hat{P}^{+}_{i\alpha}A_{qjk} \\ &\quad -\delta_{jq}<p^*_i, M\Delta^{-1}\left[\mathcal{J}(e_\alpha,\Delta p_k)+\mathcal{J}(p_k,\Delta e_\alpha)\right]> \\ &\quad -\delta_{kq}<p^*_i, M\Delta^{-1}\left[\mathcal{J}(e_\alpha,\Delta p_j)+\mathcal{J}(p_j,\Delta e_\alpha)\right]> \end{aligned} \tag{103}$$

$$\frac{\partial B_{ij}}{\partial \hat{P}_{\alpha q}} = -<\frac{\partial p_i^*}{\partial \hat{P}_{\alpha q}}, M\left(\Delta^{-1}\left[\mathcal{J}(\overline{\Psi},\Delta p_j)+\mathcal{J}(p_j,\Delta\overline{\Psi}+f+h)\right]+\kappa_1 p_j+\kappa_2\Delta^3 p_j\right)>$$
$$-\delta_{jq}<p_i^*, M\left(\Delta^{-1}\left[\mathcal{J}(\overline{\Psi},\Delta e_\alpha)+\mathcal{J}(e_\alpha,\Delta\overline{\Psi}+f+h)\right]+\kappa_1 e_\alpha+\kappa_2\Delta^3 e_\alpha\right)>$$
$$= D_{iq}^{-1}\left(\Upsilon_{\alpha j}-\sum_l \hat{P}_{\alpha l}B_{lj}\right)-\hat{P}^+_{i\alpha}B_{qj}$$
$$-\delta_{jq}<p_i^*, M\left(\Delta^{-1}\left[\mathcal{J}(\overline{\Psi},\Delta e_\alpha)+\mathcal{J}(e_\alpha,\Delta\overline{\Psi}+f+h)\right]+\kappa_1 e_\alpha+\kappa_2\Delta^3 e_\alpha\right)> \quad (104)$$

$$\frac{\partial C_i}{\partial \hat{P}_{\alpha q}} = <\frac{\partial p_i^*}{\partial \hat{P}_{\alpha q}}, M\left(\tilde{\Psi}-\Delta^{-1}\mathcal{J}(\overline{\Psi},\Delta\overline{\Psi}+f+h)-\kappa_1\overline{\Psi}-\kappa_2\Delta^3\overline{\Psi}\right)>$$
$$= D_{iq}^{-1}\left(C_\alpha^{\mathrm{eof}}-\sum_l \hat{P}_{\alpha l}C_l\right)-\hat{P}^+_{i\alpha}C_q \quad (105)$$

with

$$\Lambda_{\alpha jk} = -<e_\alpha, M\Delta^{-1}\left[\mathcal{J}(p_j,\Delta p_k)+\mathcal{J}(p_k,\Delta p_j)\right]> \quad (106)$$

$$\Upsilon_{\alpha j} = -<e_\alpha, M\left(\Delta^{-1}\left[\mathcal{J}(\overline{\Psi},\Delta p_j)+\mathcal{J}(p_j,\Delta\overline{\Psi}+f+h)\right]+\kappa_1 p_j+\kappa_2\Delta^3 p_j\right)> \quad (107)$$

As with the coefficients themselves there exist two ways of calculating the derivatives numerically. On the one hand again one can calculate all remaining Jacobians in the formulae (103) and (104) in the basis of spherical harmonics using the transform method. The other possibility is direct summation in EOF-space using the identities

$$-<p_i^*, M\Delta^{-1}\left[\mathcal{J}(e_\alpha,\Delta p_j)+\mathcal{J}(p_j,\Delta e_\alpha)\right]> = \sum_{\beta,\gamma}\hat{P}^+_{i\beta}\hat{P}_{\gamma j}A^{\mathrm{eof}}_{\beta\alpha\gamma} \quad (108)$$

and

$$-<p_i^*, M\left(\Delta^{-1}\left[\mathcal{J}(\overline{\Psi},\Delta e_\alpha)+\mathcal{J}(e_\alpha,\Delta\overline{\Psi}+f+h)\right]+\kappa_1 e_\alpha+\kappa_2\Delta^3 e_\alpha\right)> = \sum_\beta \hat{P}^+_{i\beta}B^{\mathrm{eof}}_{\beta\alpha}\,. \quad (109)$$

The former method involves $\mathcal{O}(N^{\frac{3}{2}})$ operations for each Jacobian, the latter one $\mathcal{O}(S^2)$ operations each and again storage of $\mathcal{O}(S^3)$ interaction coefficients. Hence the former method becomes more and more advantageous if S increases, but the limit is higher then in the case of the coefficients themselves. It is found to be roughly $S \approx 100$.

If the components of B are determined from $\frac{\partial Q}{\partial B_{pq}} = 0$ their derivatives are not required (cf. eq. (94)).

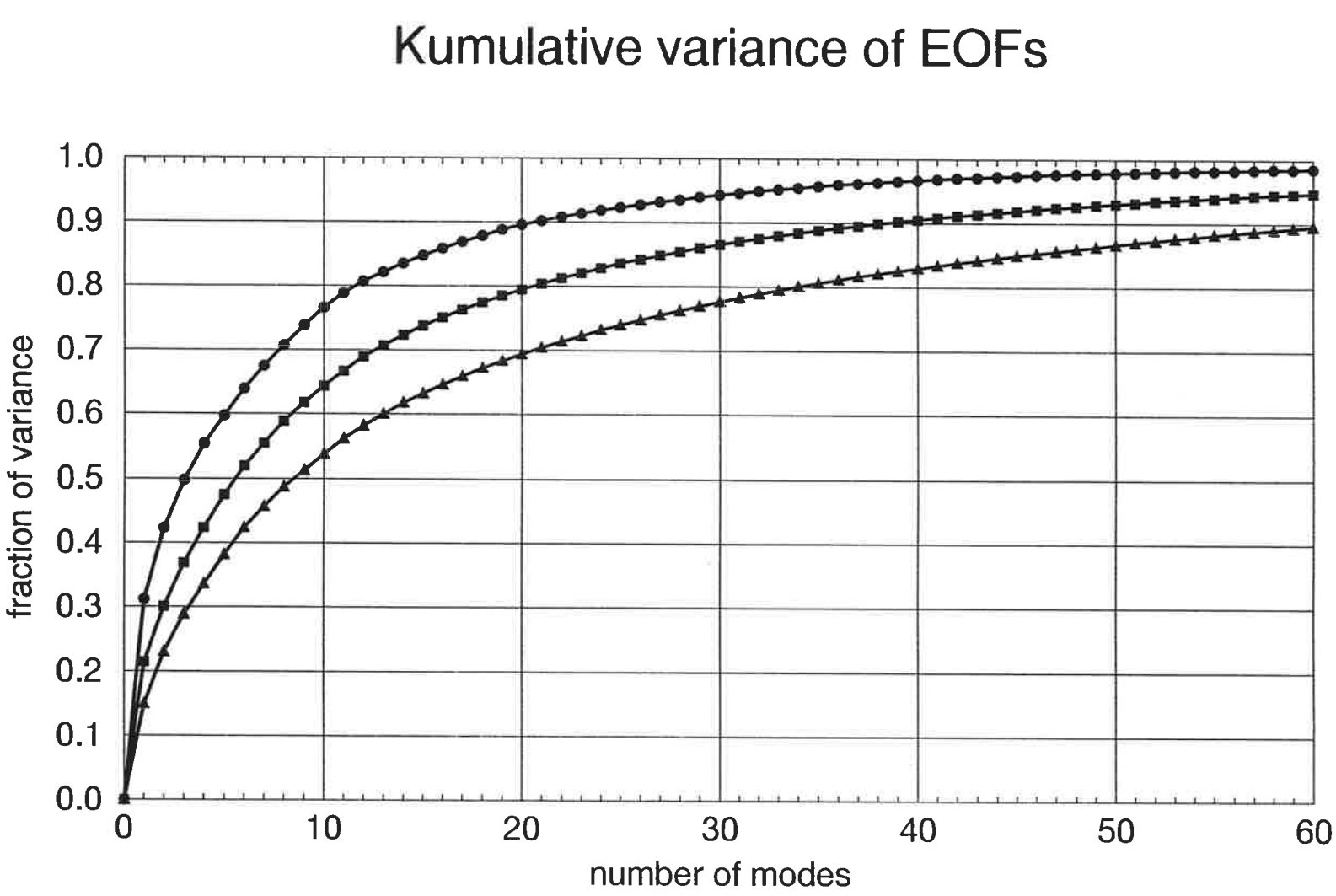

Fig. 1 : Fraction of variance captured in an expansion using the first S EOFs with respect to the norm anomaly streamfunction (circles), turbulent kinetic energy (squares) and turbulent enstrophy metric (triangles)

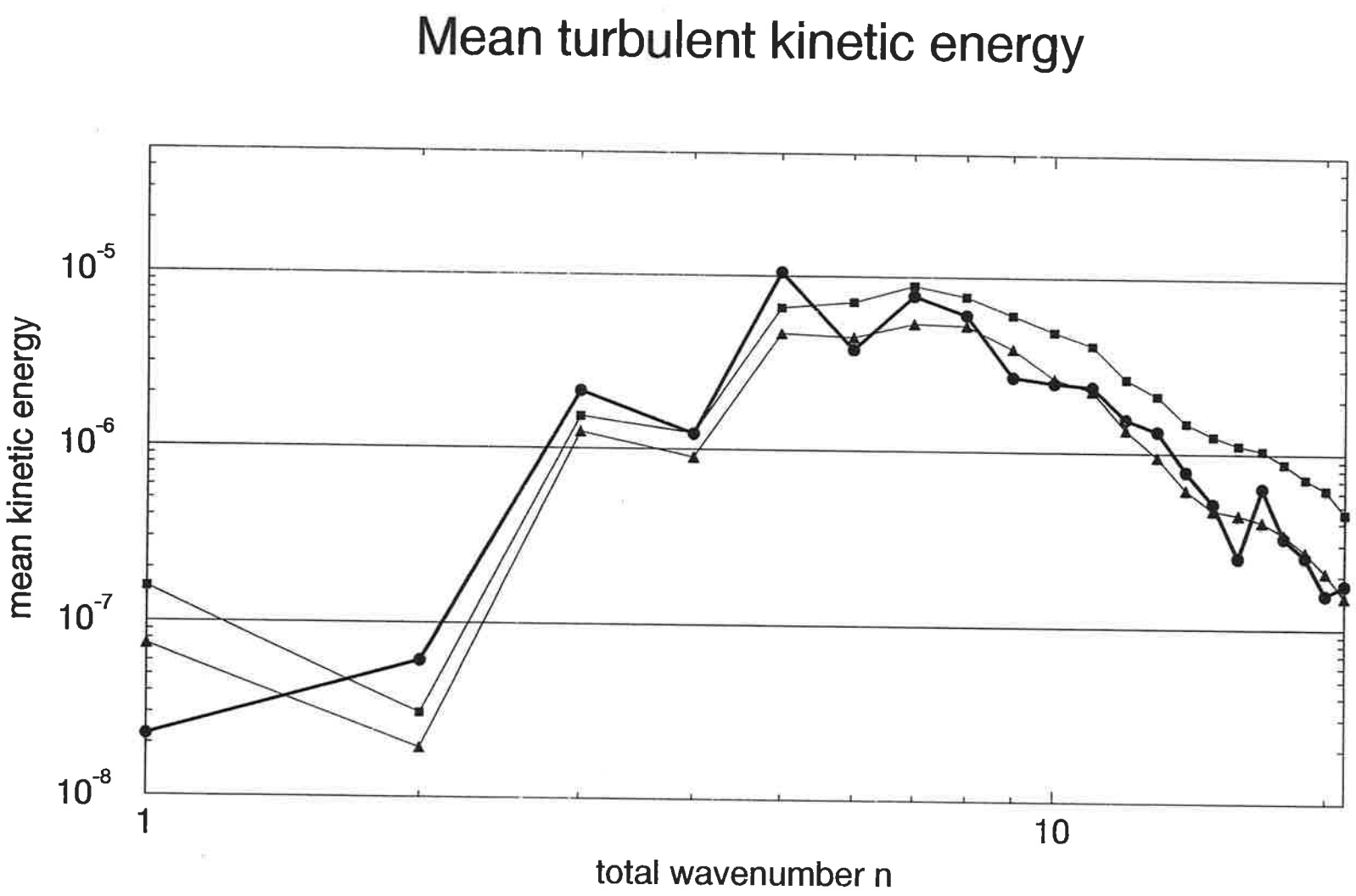

Fig. 2 : Energy spectrum of the complete system (upper thin line, squares), of the complete system projected onto the subspace of 12 PIPs (lower thin line, triangles) and of the reduced system using 12 PIPs without additional damping (thick line, circles)

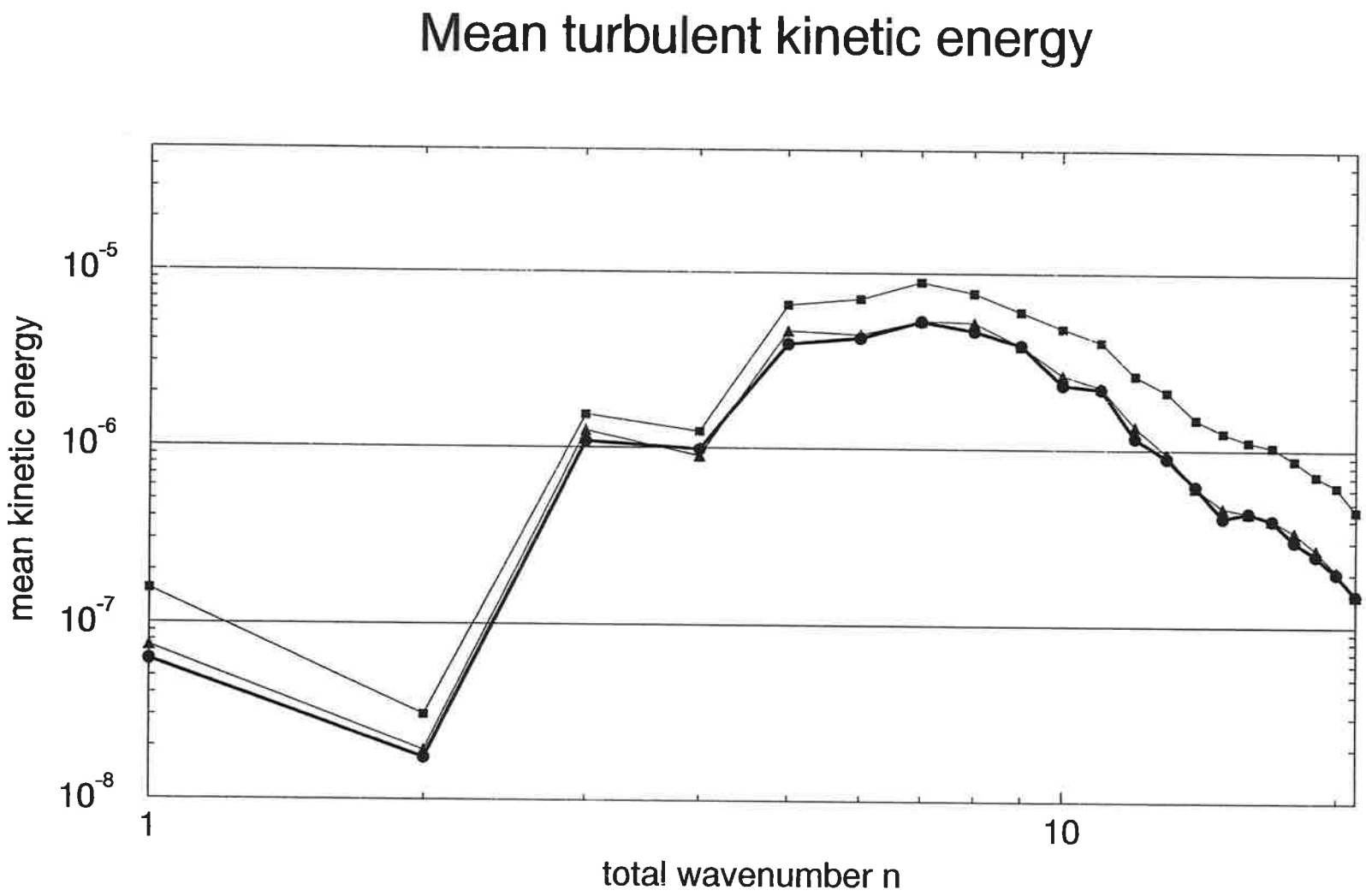

Fig. 3 : Energy spectrum of the complete system (upper thin line, squares), of the complete system projected onto the subspace of 12 PIPs (lower thin line, triangles) and of the reduced system using 12 PIPs with additional damping (thick line, circles)

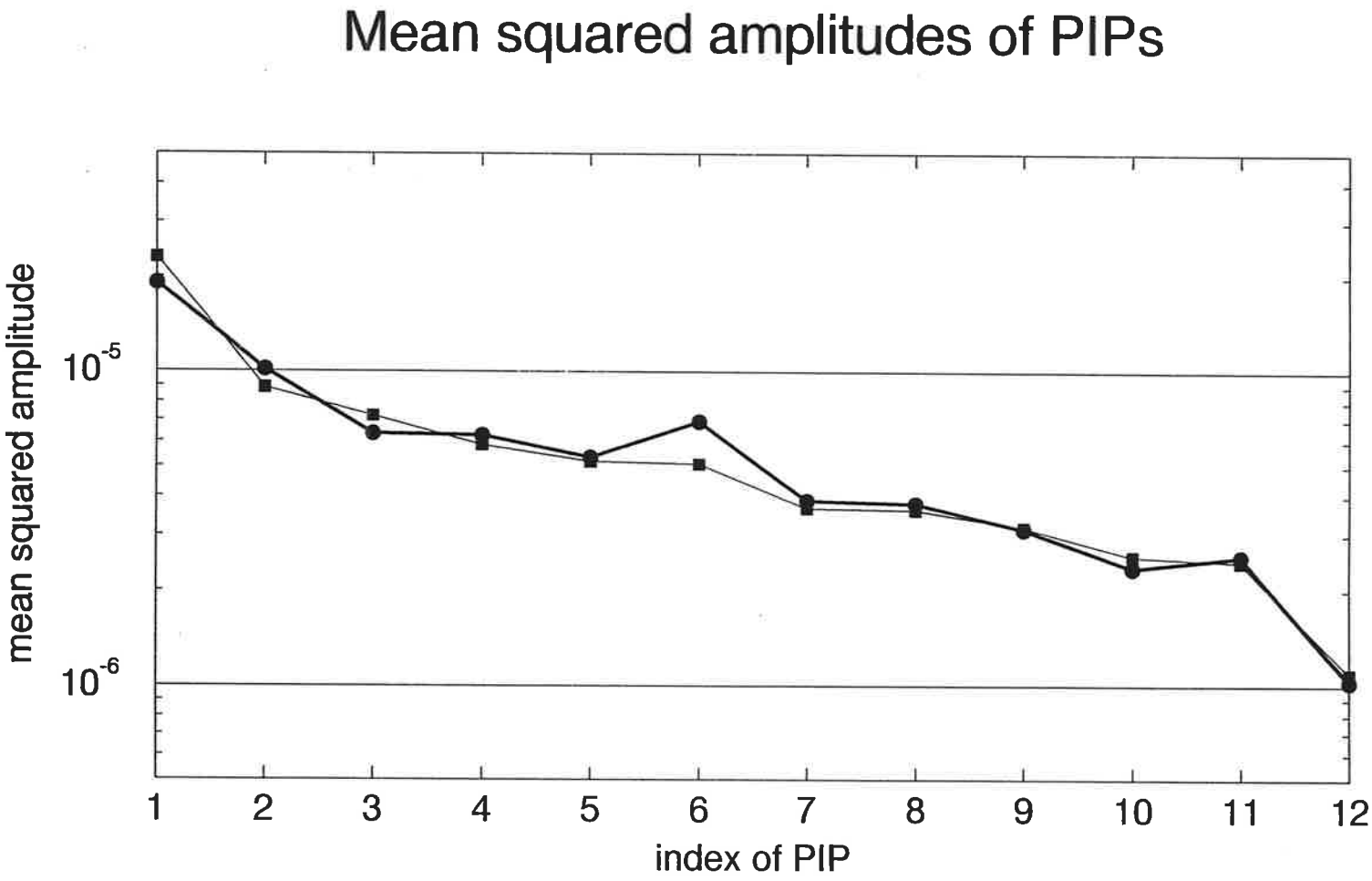

Fig. 4 : Mean squared PIP-amplitudes obtained from the reduced system with 12 modes (thick line, circles) and from the complete system (thin line, squares)

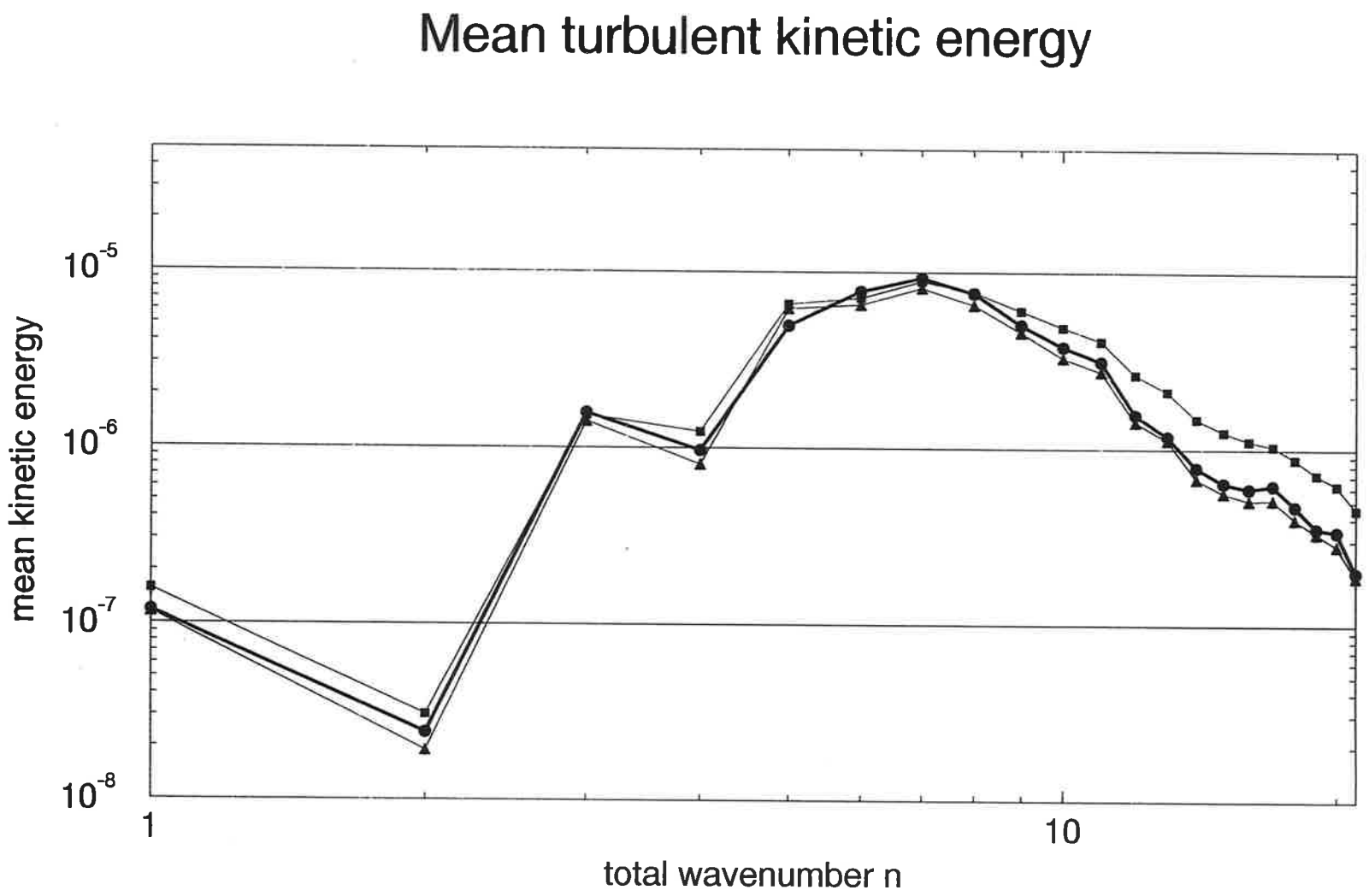

Fig. 5 : Energy spectrum of the complete system (upper thin line, squares), of the complete system projected onto the subspace of 17 EOFs (lower thin line, triangles) and of the reduced system using 17 EOFs (thick line, circles)

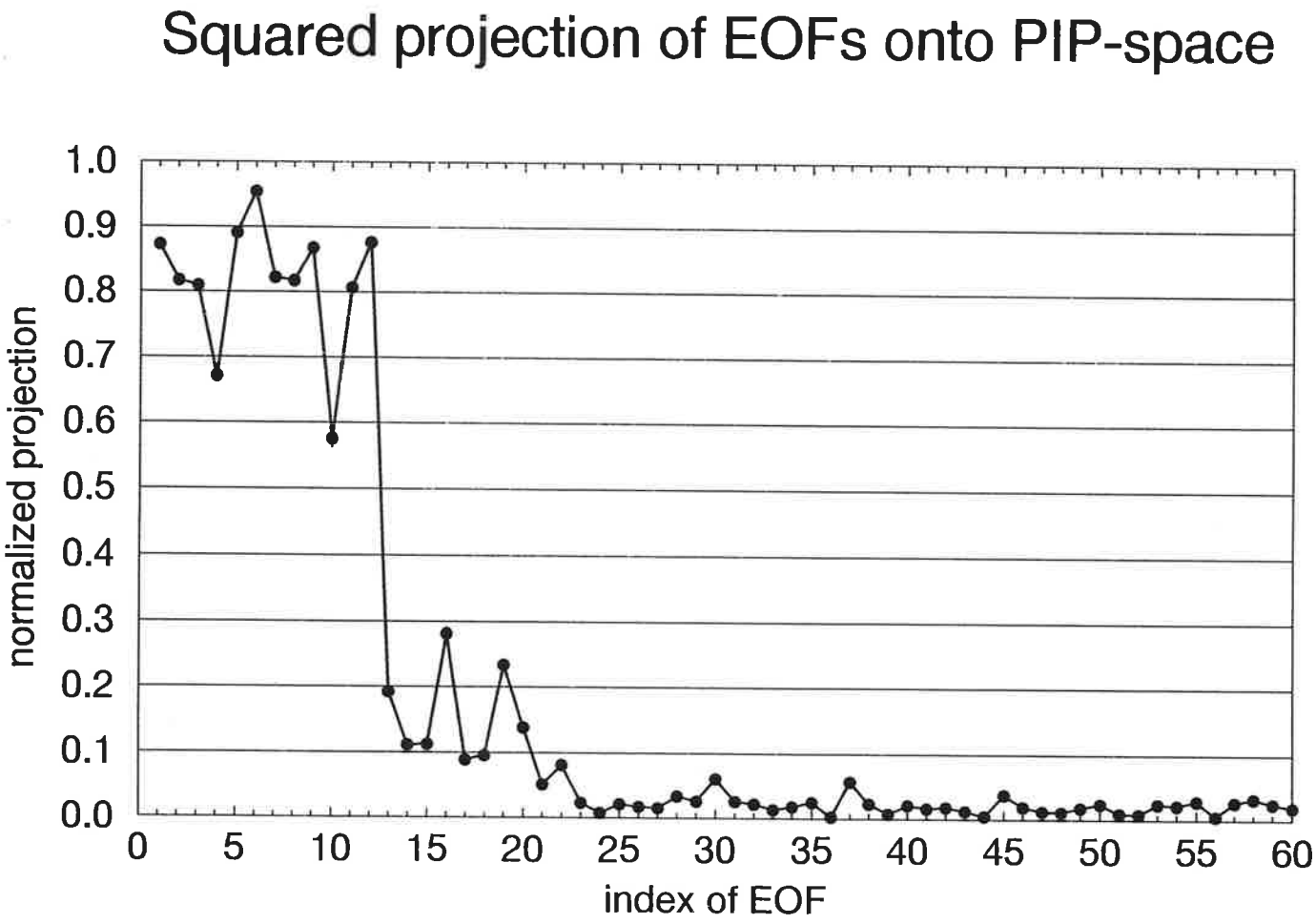

Fig. 6 : Normalized projection of EOFs onto PIP-space

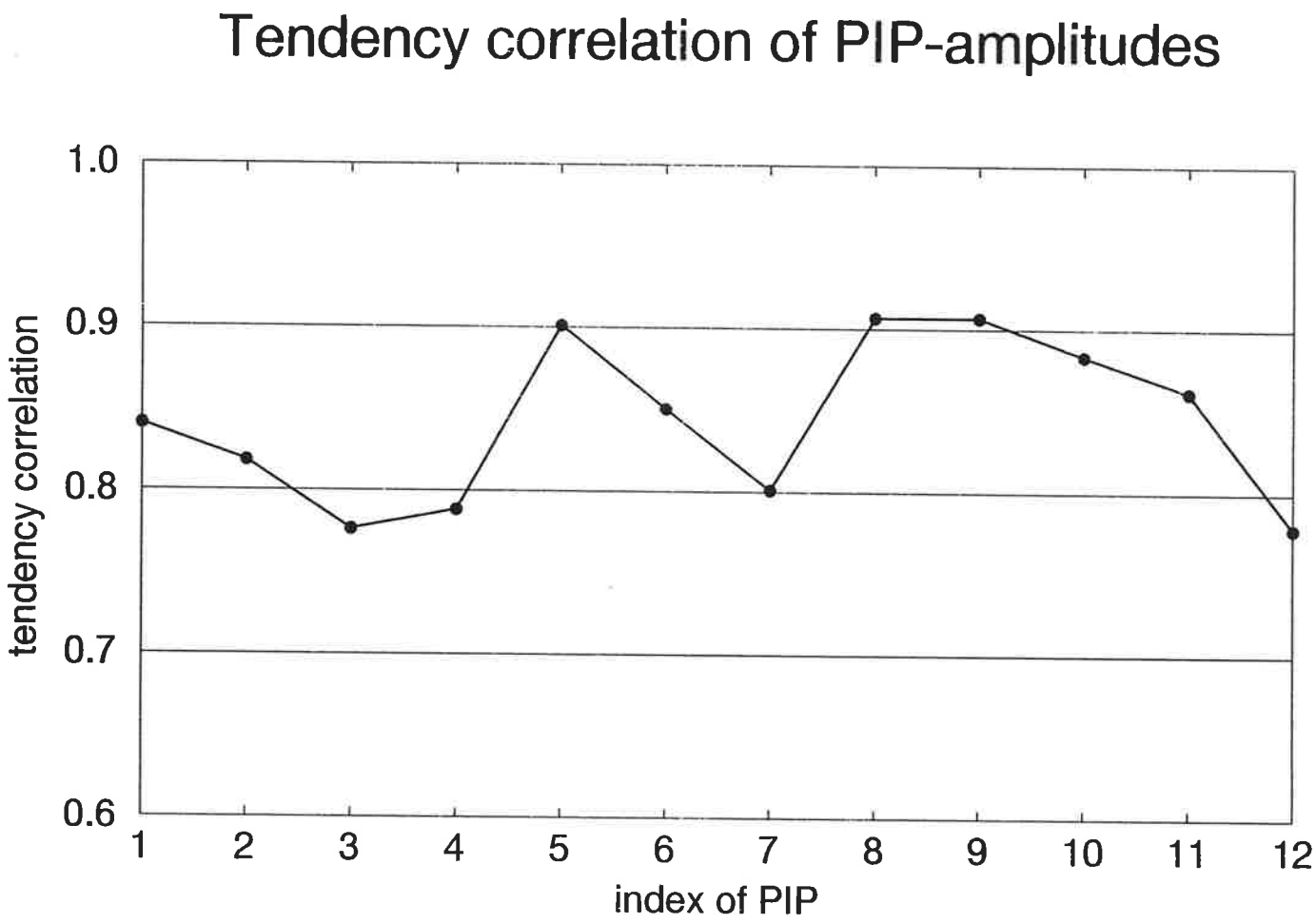

Fig. 7a : Correlations between tendencies of PIP-amplitudes given by the complete model and the reduced model using 12 PIPs

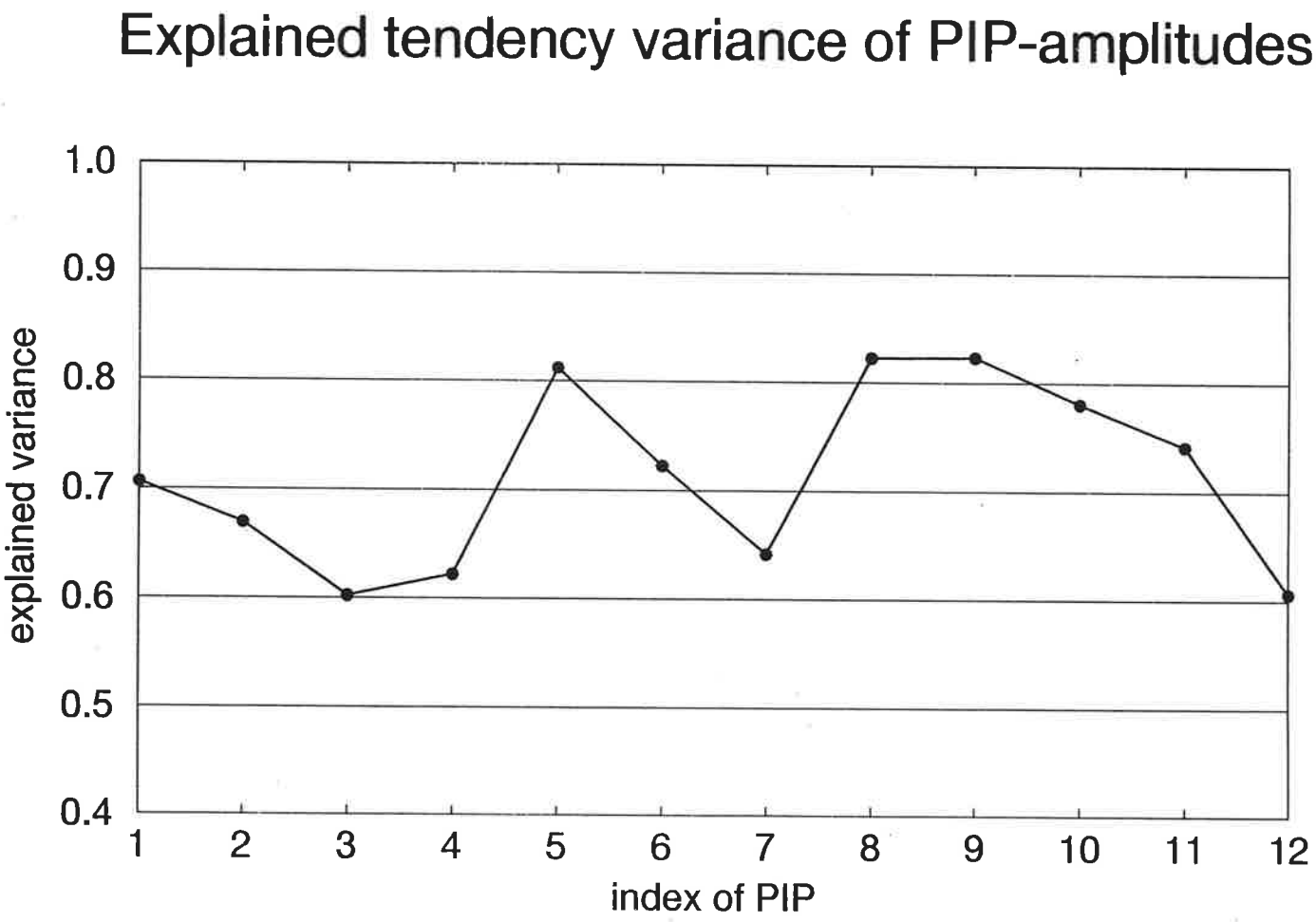

Fig. 7b : Explained tendency variance of PIP-amplitudes for the reduced model using 12 PIPs

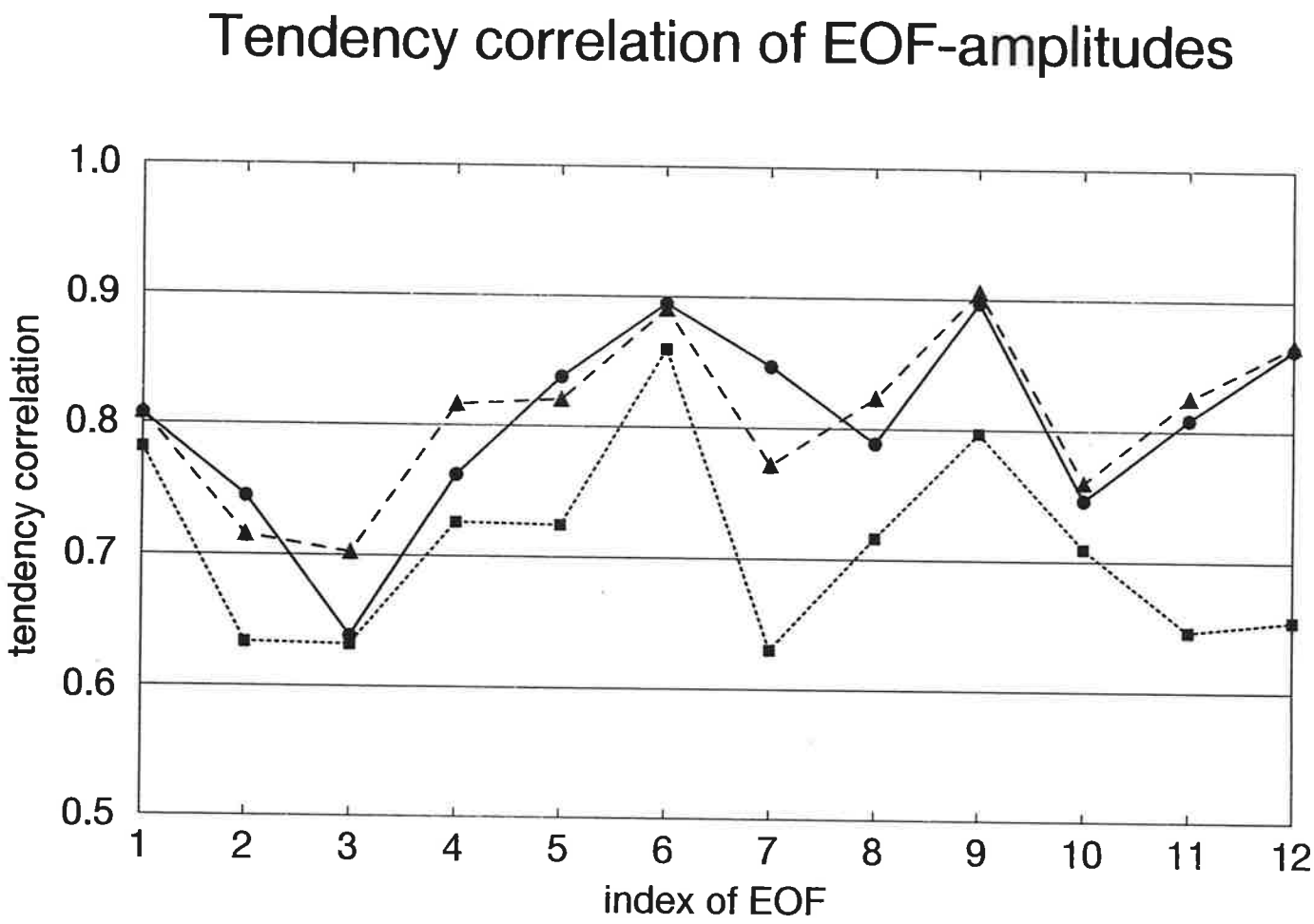

Fig. 8a : Correlation between tendencies of EOF-amplitudes given by the full model and by a reduced model using 12 EOFs (dotted line, squares), 17 EOFs (dashed line, triangles) and 12 PIPs (solid line, circles)

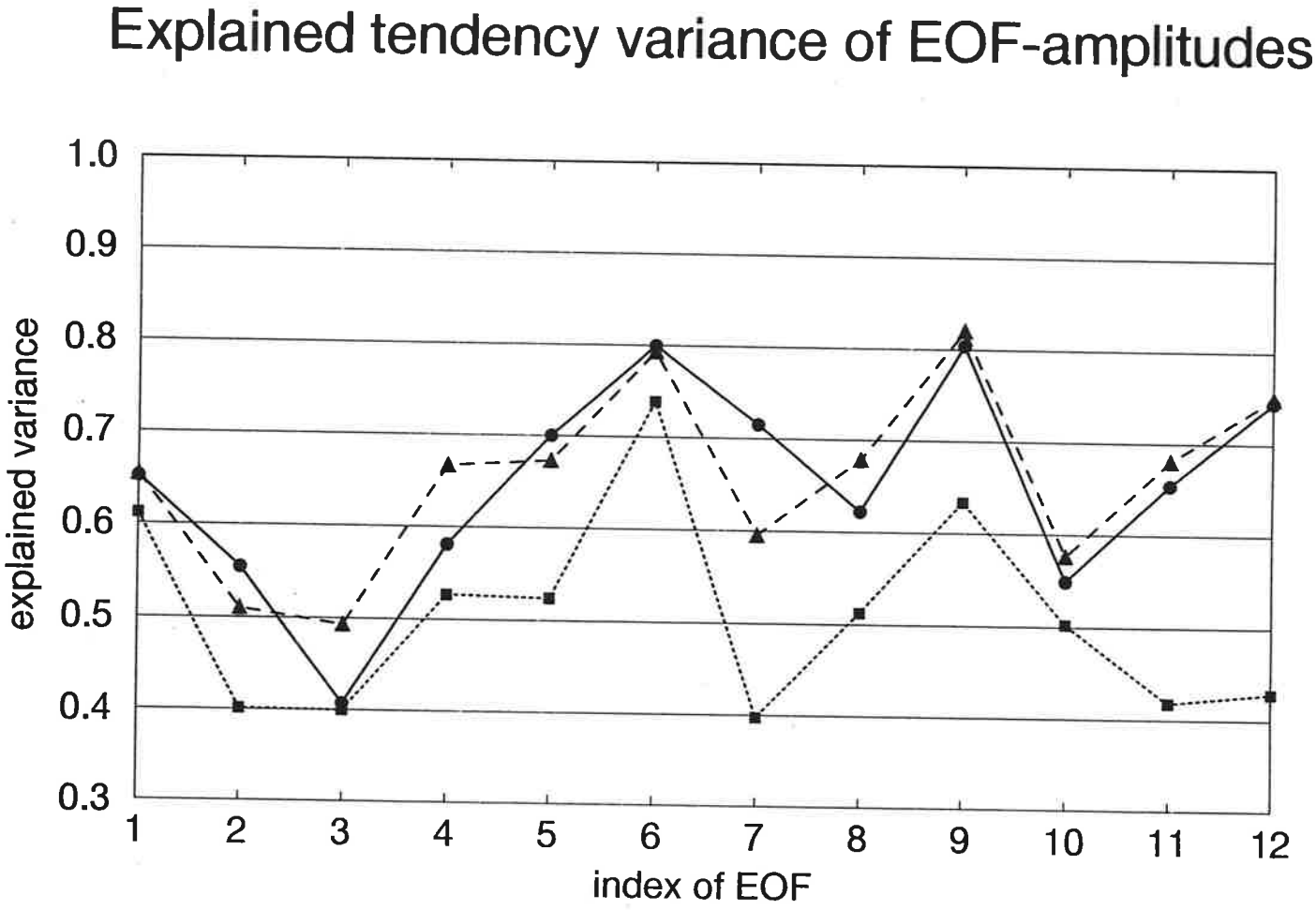

Fig. 8b : Explained tendency variance of EOF-amplitudes for a reduced model using 12 EOFs (dotted line, squares), 17 EOFs (dashed line, triangles) and 12 PIPs (solid line, circles)

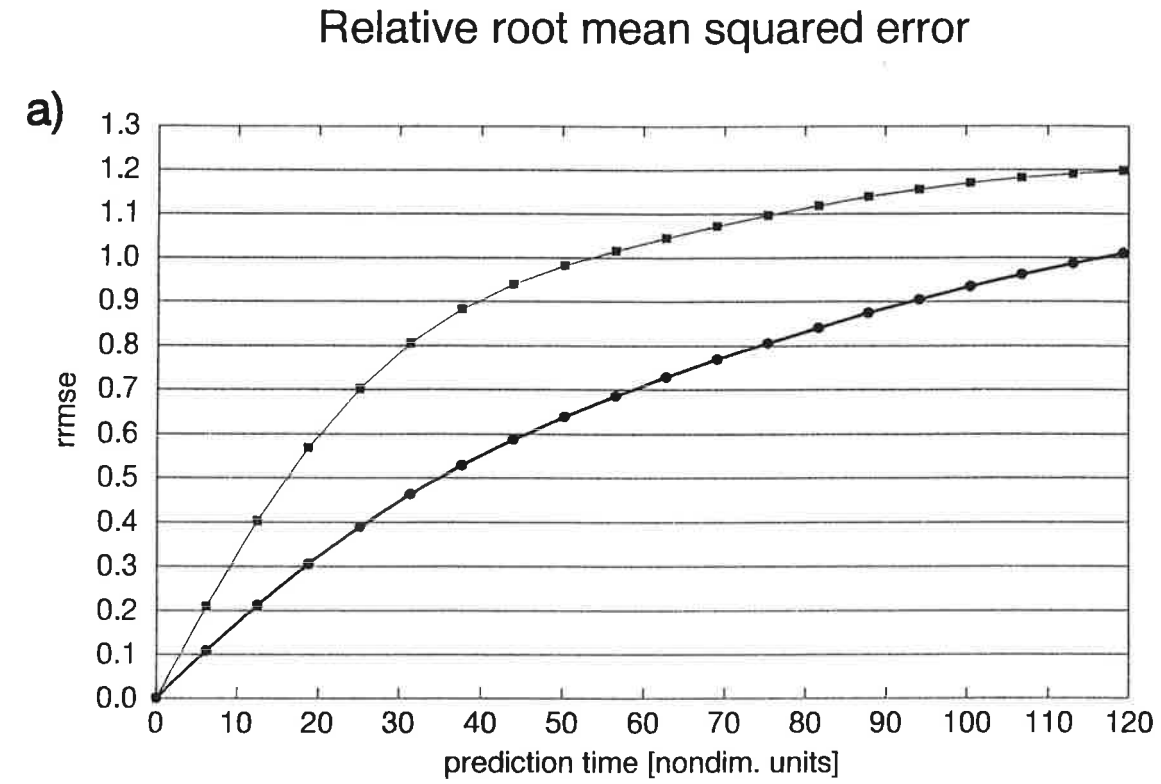

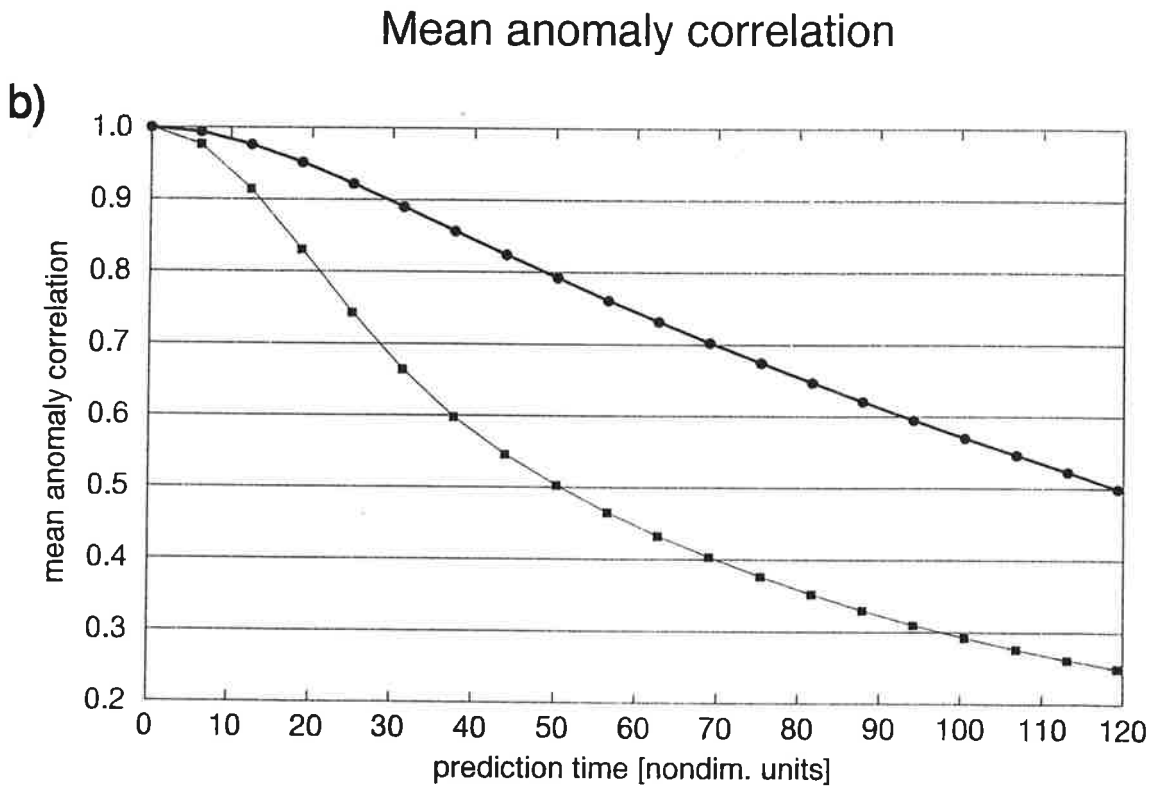

Fig. 9 : Skill of the PIP-model using 12 modes in predicting the PIP-amplitudes (thick line, circles) measured by the mean anomaly correlation (a) and by the relative root mean squared error (b) as a function of prediction time. The persistence is indicated as a control forecast (thin line, squares). Predictions start from full initial conditions.

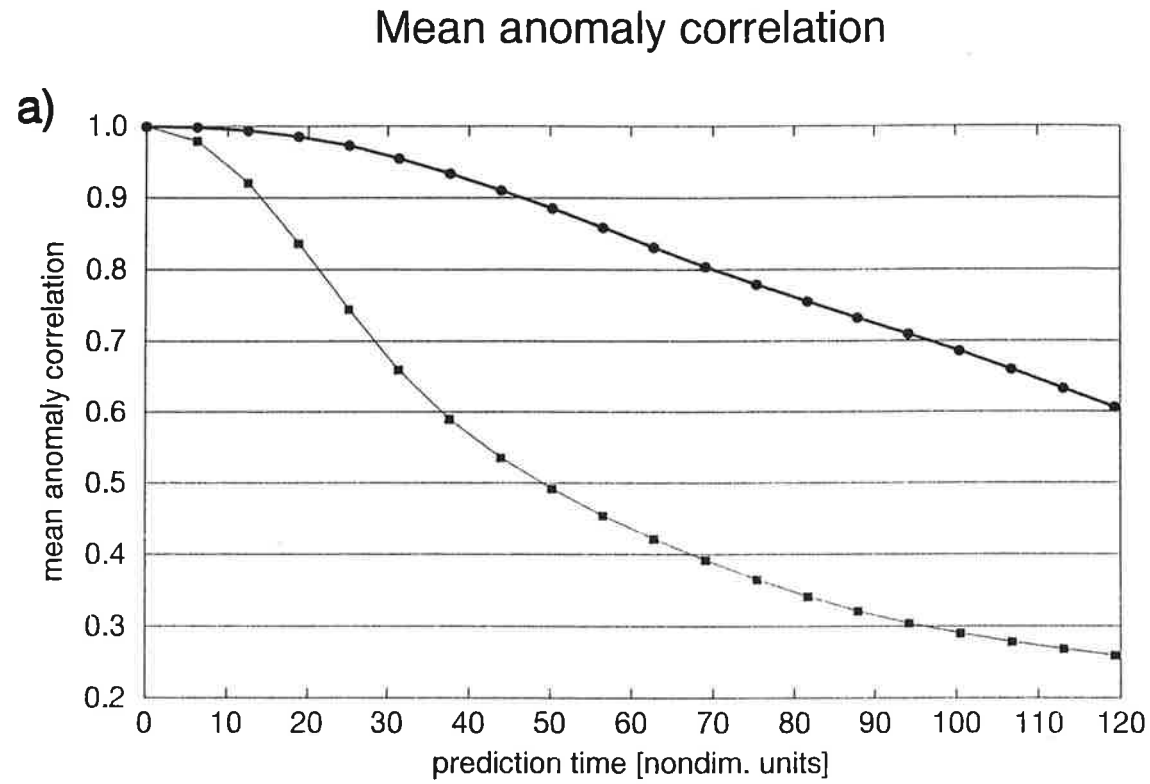

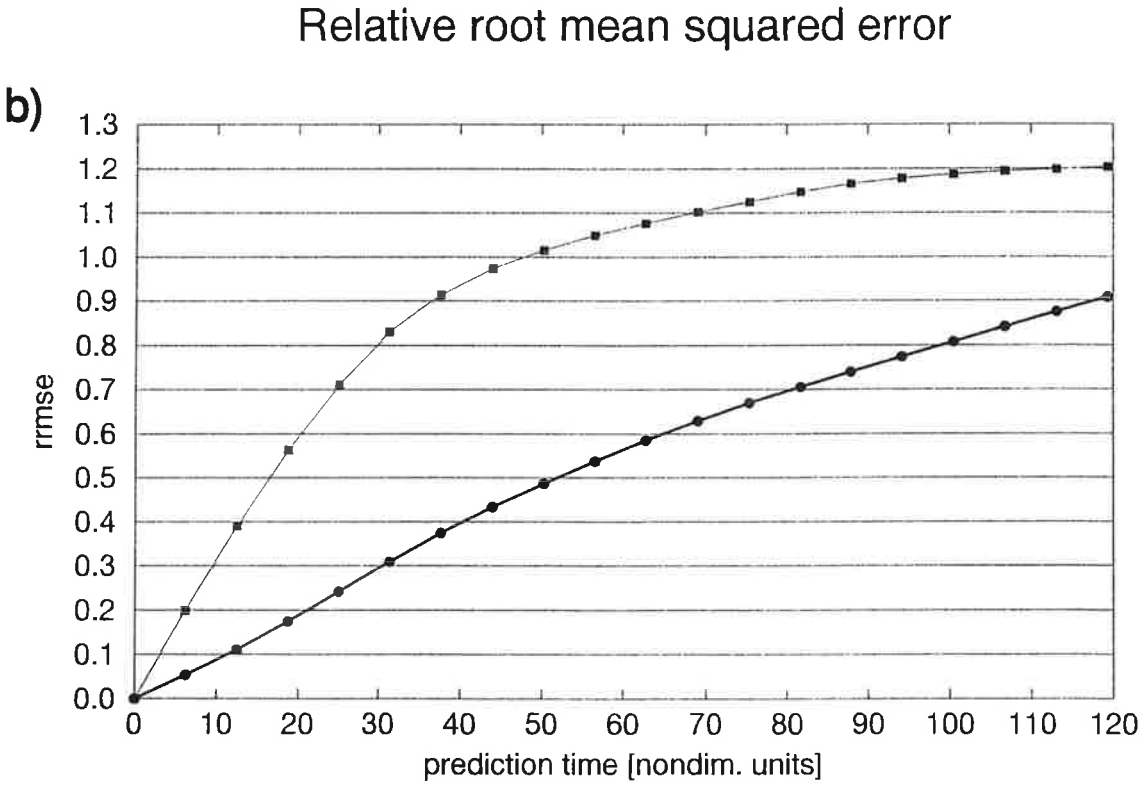

Fig. 10 : Same as Fig. 9, but with initial conditions projected onto PIP-space

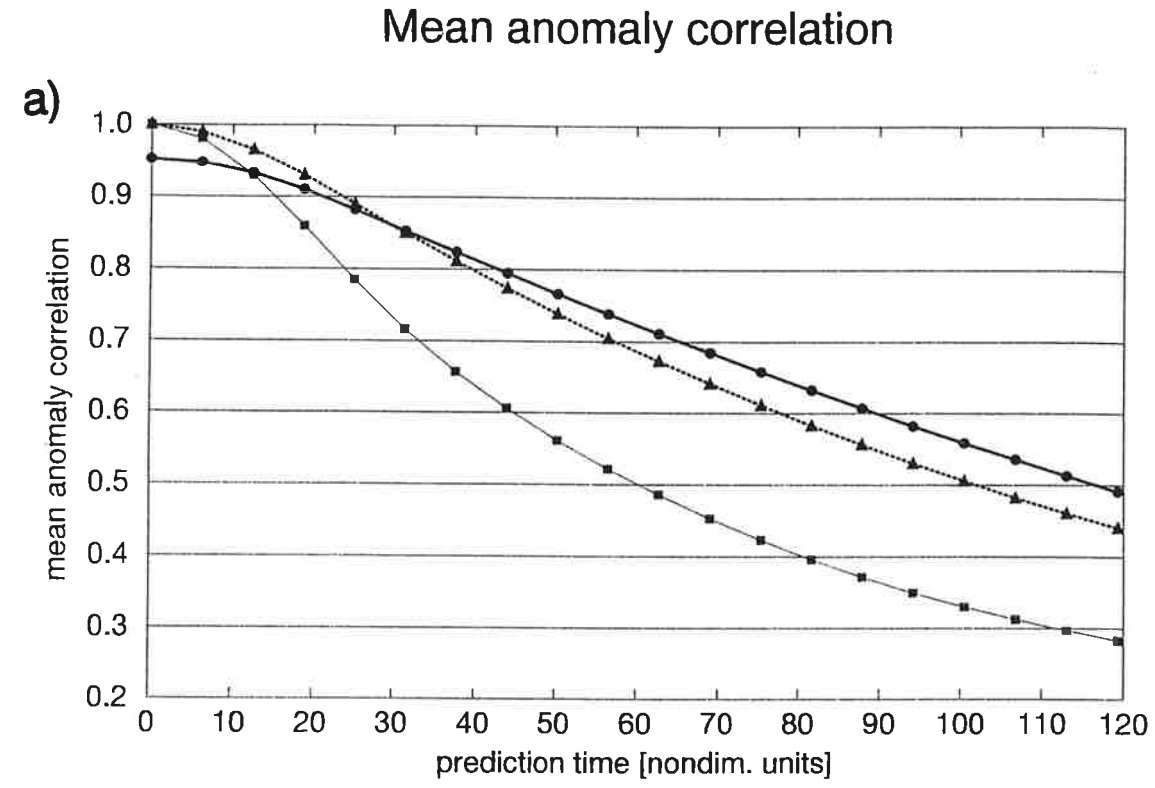

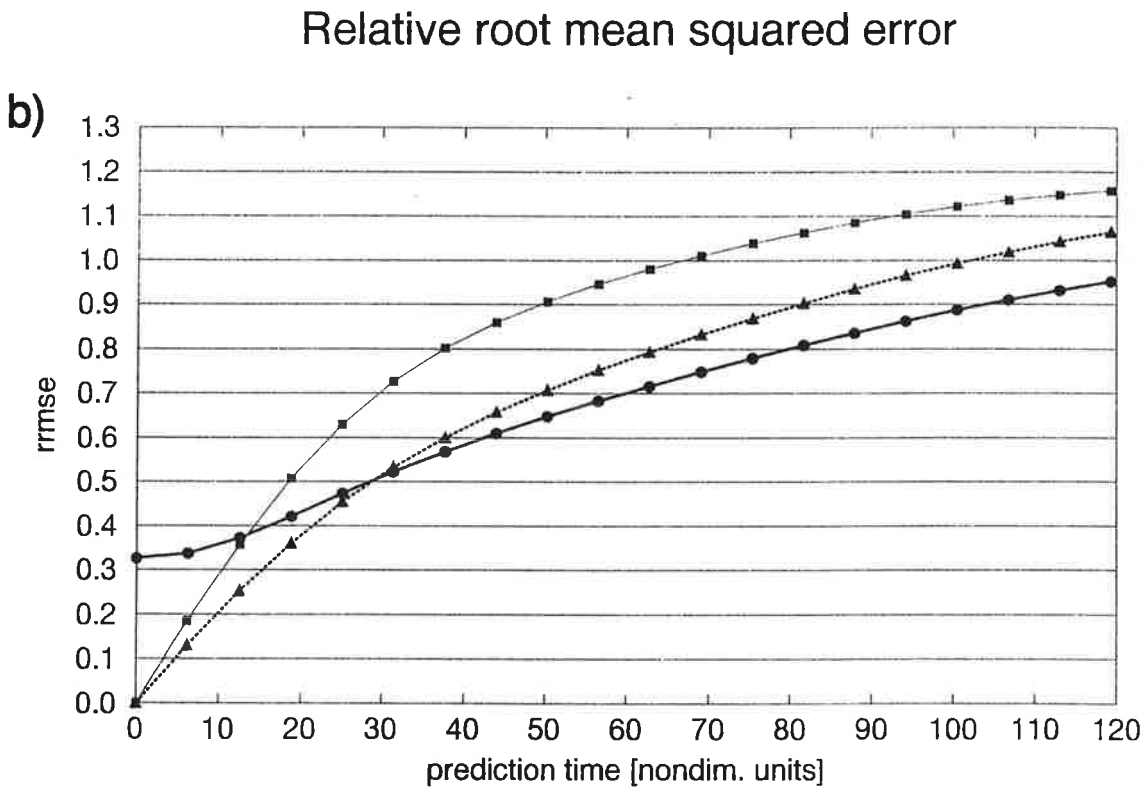

Fig. 11 : Skill of a reduced model using 12 EOFs (dotted line, triangles) and 12 PIPs (solid line, circles) in predicting the amplitudes of the first 12 EOFs measured by the mean anomaly correlation (a) and the relative root mean squared error (b) as a function of prediction time. The persistence is indicated as a control forecast (thin line, squares). Predictions start from full initial conditions.

Table Captions

Table 1 : Correlation matrix of PIP-amplitudes obtained from a long-term simulation with a PIP-model using 12 patterns

	1	2	3	4	5	6	7	8	9	10	11	12
1	1.00	0.07	0.20	0.17	0.00	-0.02	0.32	0.09	-0.05	0.15	0.03	0.03
2		1.00	0.15	0.09	-0.07	-0.02	-0.14	0.22	-0.02	-0.04	-0.11	-0.16
3			1.00	0.04	-0.12	0.06	-0.09	0.02	0.00	-0.02	-0.07	-0.07
4				1.00	0.11	0.09	0.19	0.08	0.00	0.03	0.18	0.05
5					1.00	-0.10	0.03	-0.13	0.15	-0.02	0.18	0.13
6						1.00	-0.06	0.08	-0.17	0.05	0.19	0.10
7							1.00	0.04	-0.03	0.02	0.10	0.05
8								1.00	-0.15	0.00	-0.08	-0.16
9									1.00	0.14	-0.06	0.03
10										1.00	-0.09	0.08
11											1.00	0.12
12												1.00